

## RESEARCH OUTPUTS / RÉSULTATS DE RECHERCHE

### Regulation of Bacterial Cell Cycle Progression by Redundant Phosphatases

Coppine, Jérôme; Kaczmarczyk, Andreas; Petit, Kenny; Brochier, Thomas; Jenal, Urs; Hallez, Regis

*Published in:*  
Journal of Bacteriology

*DOI:*  
[10.1128/JB.00345-20](https://doi.org/10.1128/JB.00345-20)

*Publication date:*  
2020

*Document Version*  
Peer reviewed version

#### [Link to publication](#)

*Citation for published version (HARVARD):*

Coppine, J, Kaczmarczyk, A, Petit, K, Brochier, T, Jenal, U & Hallez, R 2020, 'Regulation of Bacterial Cell Cycle Progression by Redundant Phosphatases', *Journal of Bacteriology*, vol. 202, no. 17, e00345-20.  
<https://doi.org/10.1128/JB.00345-20>

#### General rights

Copyright and moral rights for the publications made accessible in the public portal are retained by the authors and/or other copyright owners and it is a condition of accessing publications that users recognise and abide by the legal requirements associated with these rights.

- Users may download and print one copy of any publication from the public portal for the purpose of private study or research.
- You may not further distribute the material or use it for any profit-making activity or commercial gain
- You may freely distribute the URL identifying the publication in the public portal ?

#### Take down policy

If you believe that this document breaches copyright please contact us providing details, and we will remove access to the work immediately and investigate your claim.

1 **Regulation of bacterial cell cycle progression by redundant**  
2 **phosphatases**

3  
4 Jérôme Coppine<sup>1</sup>, Andreas Kaczmarczyk<sup>2</sup>, Kenny Petit<sup>1,§</sup>, Thomas Brochier<sup>1,†</sup>, Urs  
5 Jenal<sup>2</sup> and Régis Hallez<sup>1,3,4#</sup>

6  
7 <sup>1</sup> *Bacterial Cell cycle & Development (BCcD), Biology of Microorganisms Research*  
8 *Unit (URBM), Namur Research Institute for Life Science (NARILIS), University of*  
9 *Namur, Namur (5000), Belgium*

10 <sup>2</sup> *Infection Biology, Biozentrum, University of Basel, Klingelbergstrasse 50, CH-4056*  
11 *Basel, Switzerland.*

12 <sup>3</sup> *Namur Research College (NARC), University of Namur, Namur (5000), Belgium*

13 <sup>4</sup> *WELBIO, University of Namur, Namur (5000), Belgium*

14  
15 <sup>§</sup> *Present address: Department of Microbiology and Immunology, McGill University,*  
16 *Montreal, QC, Canada*

17 <sup>†</sup> *Present address: Max Planck Institute of Molecular Cell Biology and Genetics,*  
18 *Dresden, Germany*

19  
20  
21  
22 #Corresponding author: Tel: +32 81 724 244; E-mail: [regis.hallez@unamur.be](mailto:regis.hallez@unamur.be)

23  
24 Running title: Phosphatase-dependent control of bacterial cell cycle

25  
26 Key words: Two-component system, phosphorelay, phosphatase, cell cycle

27

## 28 **Abstract**

29 In the model organism *Caulobacter crescentus*, a network of two-component systems  
30 involving the response regulators CtrA, DivK and PleD coordinate cell cycle  
31 progression with differentiation. Active phosphorylated CtrA prevents chromosome  
32 replication in G1 cells while simultaneously regulating expression of genes required  
33 for morphogenesis and development. At the G1-S transition, phosphorylated DivK  
34 (DivK~P) and PleD (PleD~P) accumulate to indirectly inactivate CtrA, which triggers  
35 DNA replication initiation and concomitant cellular differentiation. The phosphatase  
36 PleC plays a pivotal role in this developmental program by keeping DivK and PleD  
37 phosphorylation levels low during G1, thereby preventing premature CtrA  
38 inactivation. Here, we describe CckN as a second phosphatase akin to PleC that  
39 dephosphorylates DivK~P and PleD~P in G1 cells. However, in contrast to PleC, no  
40 kinase activity was detected with CckN. The effects of CckN inactivation are largely  
41 masked by PleC, but become evident when PleC and DivJ, the major kinase for DivK  
42 and PleD, are absent. Accordingly, mild overexpression of *cckN* restores most  
43 phenotypic defects of a *pleC* null mutant. We also show that CckN and PleC are  
44 proteolytically degraded in a ClpXP-dependent way before the onset of the S phase.  
45 Surprisingly, known ClpX adaptors are dispensable for PleC and CckN proteolysis,  
46 raising the possibility that as yet unidentified proteolytic adaptors could be required  
47 for the degradation of both phosphatases. Since *cckN* expression is induced in  
48 stationary phase, depending on the stress alarmone (p)ppGpp, we propose that  
49 CckN acts as an auxiliary factor responding to environmental stimuli to modulate  
50 CtrA activity under suboptimal conditions.

51

## 52 **Importance**

53 Two-component signal transduction systems are widely used by bacteria to  
54 adequately respond to environmental changes by adjusting cellular parameters,  
55 including cell cycle. In *Caulobacter crescentus*, PleC acts as a phosphatase that  
56 indirectly protects the response regulator CtrA from premature inactivation during the  
57 G1 phase of the cell cycle. Here, we provide genetic and biochemical evidence that  
58 PleC is seconded by another phosphatase, CckN. The activity of PleC and CckN  
59 phosphatases is restricted to G1 phase since both proteins are timely degraded by  
60 ClpXP protease before the G1-S transition. Degradation is independent of any known

61 proteolytic adaptors and relies, in the case of CckN, on an unsuspected N-terminal  
62 degron. Our work illustrates a typical example of redundant functions between two-  
63 component proteins.

64

## 65 Introduction

66 The  $\alpha$ -proteobacterium *Caulobacter crescentus* divides asymmetrically to generate  
67 two daughter cells with different cell fates, a sessile stalked cell and a motile swarmer  
68 cell. While the newborn stalked cell can immediately re-enter S phase and initiate  
69 chromosome replication, the smaller swarmer cell engages in an obligatory motile  
70 and chemotactic but non-replicative G1 phase. Concomitantly with its entry into the S  
71 phase (G1-S transition), the swarmer cell differentiates into a stalked cell (swarmer-  
72 to-stalked cell transition). A complex regulatory network controlling the activity of the  
73 central and essential response regulator CtrA coordinates different cell cycle stages  
74 with accompanying morphological changes and development. CtrA activity is  
75 carefully regulated throughout the cell cycle at the transcriptional and post-  
76 translational levels. CtrA protein levels and its phosphorylation status are mostly  
77 determined by the action of a phosphorelay involving the hybrid kinase CckA and its  
78 cognate histidine phosphotransferase ChpT (1-4). In the swarmer cell, the kinase  
79 activity of CckA is stimulated at the flagellated pole by the physical contact with the  
80 non-conventional histidine kinase DivL (5-8). DivL is free to activate CckA since its  
81 inhibitor – the response regulator DivK – is dephosphorylated (*i.e.* inactivated) by the  
82 phosphatase PleC (PleC<sup>P</sup>). Hence, CckA promotes the ChpT-dependent  
83 phosphorylation of CtrA, thereby stimulating its activity. At the same time, the  
84 CckA/ChpT phosphorelay also protects CtrA from its proteolytic degradation by  
85 phosphorylating CpdR, a response regulator whose unphosphorylated form primes  
86 the ClpXP protease for CtrA degradation (4, 9). Active CtrA (CtrA~P) binds the single  
87 chromosomal origin of replication ( $C_{ori}$ ) to prevent DNA replication initiation (Figure  
88 1a). As a transcription factor, CtrA~P also directly activates or represses the  
89 expression of more than 200 genes involved in multiple biological processes  
90 including cell cycle, cell differentiation and cell division (10).

91 At the G1-to-S transition, DivK becomes highly phosphorylated. This results  
92 from (i) a switch from PleC phosphatase to kinase activity before proteolytic removal  
93 of PleC and (ii) post-translational stimulation of DivJ, the major histidine kinase  
94 responsible for DivK and PleD phosphorylation (11, 12). Once phosphorylated,  
95 DivK~P physically interacts with DivL and strongly reduces its affinity for CckA (7, 8,  
96 13). Hence, the kinase activity of CckA is no longer stimulated. Simultaneously, CckA  
97 phosphatase activity is directly stimulated by c-di-GMP, the levels of which strongly

98 and rapidly rise due to activation of the diguanylate cyclase PleD and inactivation of  
99 the phosphodiesterase PdeA. PleD becomes highly phosphorylated (*i.e.* activated)  
100 by DivJ at the differentiating pole (14, 15), whereas PdeA is degraded by ClpXP (16).  
101 High levels of c-di-GMP also drive ClpXP-dependent degradation of CtrA directly by  
102 binding to the proteolytic adaptor PopA (17, 18). Together, these events result in the  
103 rapid inactivation of CtrA during G1-S transition and trigger an irreversible program  
104 leading to chromosome replication and cell differentiation (Figure 1b). Inactivation of  
105 PleC phosphatase activity and the resulting increase in DivK~P (and PleD~P) are, to  
106 our knowledge, the earliest known events in this G1-S transition signalling pathway.  
107 We thus wondered whether other factors besides PleC and DivJ could influence DivK  
108 and PleD (de)phosphorylation.

109         Almost 20 years ago, interaction partners of DivK were identified in a yeast  
110 two-hybrid screen (13). Apart from PleC, DivJ and DivL, which were unsurprisingly  
111 found as prominent hits, another histidine kinase called CckN was discovered in this  
112 study as a physical partner of DivK (13), but the role played by this actor in the CtrA  
113 regulatory network has not been characterized in detail so far. Here we show that  
114 similarly to PleC, CckN displays phosphatase activity towards DivK and PleD during  
115 the G1/swarmer phase of the cell cycle. However, in contrast to PleC, the kinase  
116 activity of CckN cannot be activated by DivK~P at the G1-S transition. Both  
117 phosphatases are required to sustain optimal CtrA activity in the non-replicative  
118 swarmer cells before being inactivated by proteolysis at the G1-S transition.  
119 Interestingly, we also show that both CckN and PleC are the earliest CtrA regulatory  
120 proteins to concomitantly disappear, likely by ClpXP-dependent proteolysis.  
121 Surprisingly, these degradations do not rely on any known proteolytic adaptors for  
122 ClpXP. In addition, we show that *cckN* expression is stimulated in stationary phase,  
123 depending on (p)ppGpp. We propose a model in which CckN influences CtrA activity  
124 under non-optimal growth conditions.

125

## 126 Results

### 127 CckN is a second phosphatase for DivK and PleD

128 CckN was previously identified as an interaction partner of DivK in a yeast two-hybrid  
129 screen (13). The interaction of CckN with DivK was confirmed by  
130 coimmunoprecipitation (Figure 2a) and bacterial two-hybrid assays (Figure 2b). We  
131 next tested whether CckN displayed kinase activity, *i.e.* could autophosphorylate *in*  
132 *vitro* in the presence of ATP. Purified CckN with either a N-terminal His6 or a His6-  
133 MBP tag did not show autokinase activity *in vitro* in our experiments, despite the  
134 presence of a predicted HATPase domain (pfam02518) and all the catalytic residues  
135 in the DHP and CA domains conserved in prototypical HisKA-type histidine kinases  
136 (19). In contrast, we detected robust autophosphorylation of His6-MBP-tagged  
137 purified *C. crescentus* DivJ and PleC proteins encompassing the cytoplasmic  
138 catalytic histidine kinase core region as well as of His6-tagged purified DivJ  
139 comprising the soluble cytoplasmic catalytic core region from *Sinorhizobium meliloti*  
140 (DivJ<sup>Sm</sup>) (Figure 2c, Supplementary Figure 1a, b). A non-phosphorylatable variant of  
141 DivK (DivK<sub>D53N</sub>) stimulated *C. crescentus* DivJ and PleC autokinase activity, as  
142 reported before (15), but did not show any stimulatory effect on CckN  
143 autophosphorylation (Supplementary Figure 1a, b). Accordingly, DivK could be  
144 phosphorylated with the non-cognate DivJ<sup>Sm</sup>, but not with CckN. In contrast, CckN  
145 was able to efficiently dephosphorylate DivK~P, with CckN becoming simultaneously  
146 phosphorylated (Figure 2c). Since PleC and DivJ are known to also  
147 (de)phosphorylate another response regulator akin to DivK, PleD, we next tested  
148 whether CckN could dephosphorylate PleD. As shown in Figure 2d, CckN was able  
149 to rapidly dephosphorylate PleD. In the presence of DivK<sub>D53N</sub> in reactions containing  
150 DivJ and CckN, PleD dephosphorylation was still observed (Supplementary Figure  
151 1c), suggesting that in contrast to PleC (15), the kinase activity of CckN is not subject  
152 to stimulation by DivK<sub>D53N</sub>. Finally, we measured PleD~P levels *in vivo* in strains  
153 overexpressing *cckN* from a multicopy plasmid under the control of the xylose-  
154 inducible P<sub>xyIX</sub> promoter (pBX-*cckN*). In line with *in vitro* data, we found that the  
155 phosphorylated form of PleD (PleD~P) was strongly reduced upon overexpression of  
156 wild-type *cckN* compared to a control strain harbouring an empty vector, whereas  
157 overexpression of a mutant variant of *cckN* (*cckN*<sub>H47A</sub>) that has the predicted  
158 phosphorylatable His47 residue mutated to Ala did not influence PleD~P levels

159 (Figure 2e). Together, these results suggest that CckN is a phosphatase but not a  
160 kinase for both DivK and PleD.

161

### 162 **CckN impacts CtrA activity through DivK**

163 As a regulator of DivK phosphorylation, CckN is expected to affect CtrA activity. To  
164 test this hypothesis, we monitored the activity of CtrA-dependent promoters in  
165 different genetic backgrounds using *lacZ* transcriptional reporters and  $\beta$ -  
166 galactosidase assays. We found that inactivating *cckN* in an otherwise wild-type  
167 background did not substantially change CtrA activity (Supplementary Figure 2a).  
168 Likewise,  $\Delta cckN$  did not interfere with the hyper-activity of CtrA measured in a  $\Delta divJ$   
169 background (Supplementary Figure 2a). Whereas CtrA-dependent promoters  
170 displayed almost no activity in  $\Delta pleC$  cells (Supplementary Figure 2a), the  
171 concomitant inactivation of *divJ* in  $\Delta divJ \Delta pleC$  cells restored a detectable activity  
172 (Figure 3a, Supplementary Figure 2b). Interestingly, *cckN* inactivation in this  
173  $\Delta divJ \Delta pleC$  background diminished activity of CtrA-dependent promoters, with a  
174 decrease ranging from 20% to 80% depending on the promoter, but did not influence  
175 activity of promoters that are not regulated by CtrA (Figure 3a, Supplementary Figure  
176 2b). These results suggest that PleC constitutes the main phosphatase of DivK and  
177 thus needs to be inactivated – together with DivJ – to unmask the effects of CckN.  
178 We also found that  $\Delta cckN$  modulated activity of CtrA in a *pleC<sub>F778L</sub>* background  
179 (Supplementary Figure 3a). This PleC variant was described to lack kinase but not  
180 phosphatase activity (PleC<sup>K-P+</sup>) *in vitro* and was shown to complement motility, phage  
181 sensitivity and stalk biogenesis defects of a  $\Delta pleC$  mutant when expressed on a  
182 multicopy plasmid (20). However, in cells in which *pleC<sub>F778L</sub>* was expressed as the  
183 only copy from the endogenous *pleC* locus, the activity of CtrA-dependent promoters  
184 was less active than in wild-type cells, but more active than in  $\Delta pleC$  cells  
185 (Supplementary Figure 3a). These data suggest that when expressed from its native  
186 genomic context, the phosphatase activity displayed by PleC<sub>F778L</sub> is reduced  
187 compared to wild-type PleC. Accordingly, the activity of CtrA-dependent promoters  
188 was further decreased in *pleC<sub>F778L</sub> ΔcckN* cells to levels observed with fully inactive  
189 alleles of *pleC*, such as  $\Delta pleC$  or *pleC<sub>H610A</sub>* (Supplementary Figure 3a). In line with  
190 these effects, *cckN* inactivation in a *pleC<sub>F778L</sub>* background further decreased motility  
191 and attachment compared to the parental *pleC<sub>F778L</sub>* strain (Supplementary Figure 3b).

192 Together, these data support the idea that PleC masks the phosphatase activity of  
193 CckN on DivK under standard laboratory conditions.

194         Given that DivK~P negatively affects CtrA phosphorylation and protein levels  
195 (4, 21), we monitored phosphorylation and protein abundance of CtrA in  $\Delta divJ \Delta pleC$   
196 vs  $\Delta divJ \Delta pleC \Delta cckN$  cells. Whereas CtrA abundance did not vary substantially, the  
197 phosphorylation state of CtrA was strongly diminished in the triple mutant  
198 ( $\Delta divJ \Delta pleC \Delta cckN$ ) in comparison to the parental  $\Delta divJ \Delta pleC$  strain (Figure 3b).  
199 Thus, CckN impacts CtrA activity mainly by promoting its phosphorylation,  
200 presumably via dephosphorylation of DivK. Comparative chromatin  
201 immunoprecipitation experiments coupled to deep sequencing (ChIP-seq) in  
202  $\Delta divJ \Delta pleC \Delta cckN$  vs  $\Delta divJ \Delta pleC$  cells showed that *cckN* inactivation impacts the  
203 entire CtrA regulon (Supplementary Figure 3c, Supplementary Table 1).

204         Finally, we checked whether the effect of CckN on CtrA phosphorylation and  
205 activity was fully dependent on DivK by monitoring the activity of CtrA in the absence  
206 of *divK*. As *divK* is essential but was shown to be dispensable in a *cpdR<sub>D51A</sub>*  
207 background (22), we measured the activity of CtrA-regulated promoters in *cpdR<sub>D51A</sub>*  
208  $\Delta divK$  with or without *cckN*. In contrast to *divK*<sup>+</sup> cells (Figure 3a, d), inactivating *cckN*  
209 did not influence CtrA activity in the absence of DivK any further (Supplementary  
210 Figure 3d), suggesting that CckN acts on CtrA mostly – if not entirely – through DivK.  
211 Altogether, these results suggest that CckN is a phosphatase of DivK akin to PleC,  
212 ultimately keeping CtrA active in G1 cells.

213

#### 214 **CckN controls development in a CtrA-dependent way**

215 Next, we tested whether *cckN* inactivation displayed developmental defects. A  $\Delta pleC$   
216 strain is known to be fully resistant to both CbK and Cr30 bacteriophages (Figure 3c)  
217 (23, 24). This is due to *pilA* and *hvyA* transcription being directly activated by CtrA~P,  
218 and not being sufficiently expressed in the absence of PleC (Figure 3d) (24, 25). *pilA*  
219 codes for the major pilin subunit of polar pili used by phage CbK as a receptor (26).  
220 *hvyA* encodes a transglutaminase homolog that specifically protects swarmer cells  
221 from capsulation, thereby allowing the Cr30 bacteriophage to reach its receptor, the  
222 S-layer (27). Thus, neither CbK nor Cr30 can infect  $\Delta pleC$  cells since the polar pili  
223 are absent and the S-layer inaccessible. Because the differential capsulation of  
224 *Caulobacter* daughter cells is also responsible for their specific buoyancy properties,

225 with the non-capsulated swarmer cells being heavy and the other capsulated cell  
226 types light (24),  $\Delta pleC$  swarmer cells lack their typical low buoyancy feature by  
227 becoming capsulated (Figure 3e). As expected and as reported before, full resistance  
228 to both bacteriophages, high buoyancy and low  $P_{pilA}$  and  $P_{hvyA}$  activity displayed by  
229 the single  $\Delta pleC$  strain was restored by inactivating  $divJ$  (Figure 3c-e) (11, 24, 28).  
230 Interestingly, we found that a non-functional allele of  $cckN$  ( $\Delta cckN$  or  $cckN_{H47A}$ )  
231 reduced sensitivity to bacteriophages, significantly decreased the activity of  $P_{pilA}$  and  
232  $P_{hvyA}$  and lost low buoyancy in a  $\Delta divJ \Delta pleC$  or  $pleC_{F778L}$  background, but not in an  
233 otherwise wild-type background (Figure 3c-e, Supplementary Figure 3e). In line with  
234 the lower sensitivity to Cr30 infection, the relative Cr30-mediated transduction  
235 efficiency was also significantly reduced in  $\Delta divJ \Delta pleC \Delta cckN$  and  
236  $\Delta divJ \Delta pleC cckN_{H47A}$  mutants compared to the parental  $\Delta divJ \Delta pleC$  strain (Figure  
237 3f). In addition, expressing  $cckN$  from the chromosomal xylose-inducible promoter  
238  $P_{xyIX}$  could complement loss of  $cckN$  in the  $\Delta divJ \Delta pleC \Delta cckN$  mutant as sensitivity  
239 to both CbK and Cr30 infections increased upon xylose induction (Supplementary  
240 Figure 3f). Together, these data suggest that  $cckN$  controls development by  
241 sustaining optimal CtrA activity.

242

### 243 **Overexpression of $cckN$ suppresses $\Delta pleC$ defects by enhancing CtrA activity**

244 The results presented above suggested that  $cckN$  overexpression should lead to an  
245 increase of CtrA phosphorylation. To test this hypothesis,  $cckN$  was first mildly  
246 overexpressed in a  $\Delta pleC$  mutant from the endogenous  $xyIX$  locus. According to the  
247 data presented above, we found that the xylose-induced expression of  $cckN$  in a  
248  $\Delta pleC$  background ( $\Delta pleC P_{xyIX}::cckN$ ) restored sensitivity to CbK and Cr30 phages  
249 (Supplementary Figure 4a), significantly increased  $hvyA$  and  $pilA$  expression  
250 (Supplementary Figure 4b). Thus, CckN is capable of replacing PleC function under  
251 conditions where PleC is absent. However, the same mild overexpression of  $cckN$   
252 did not restore attachment of  $\Delta pleC$  cells (Supplementary Figure 4c), likely because  
253 holdfast production required for irreversible attachment essentially relies on PleC  
254 kinase rather than phosphatase activity on PleD (15). In support of this, mild  
255 overexpression of  $cckN$  in wild-type cells significantly decreased binding to abiotic  
256 surfaces likely by dephosphorylating PleD~P (Supplementary Figure 4c).  
257 Furthermore,  $cckN$  inactivation in an otherwise wild-type or a  $\Delta divJ \Delta pleC$

258 background did not significantly decrease attachment (Supplementary Figure 4d). In  
259 contrast, *cckN* inactivation in a *pleC<sub>F778L</sub>* background – which displayed a partial  
260 attachment defect compared to the complete loss of attachment of a *pleC* null mutant  
261 – led to a significant decrease of attachment (Supplementary Figure 3b). These  
262 effects could be due to the decrease of CtrA~P, which results in reduced expression  
263 of *pilA* (Supplementary Figure 3a) involved in primary attachment (29) and *hfa* genes  
264 involved in holdfast attachment (10).

265 To further characterize the role played by *cckN*, we generated a multi-copy  
266 plasmid on which *cckN* was placed under the control of the xylose-inducible  $P_{xyIX}$   
267 promoter (pBX-*cckN*). In comparison to the control wild-type strain harbouring an  
268 empty plasmid (EV), wild-type cells harbouring pBX-*cckN* were filamentous and  
269 arrested in G1 when xylose was added to the media (Figure 4a). This result suggests  
270 that a strong overexpression of *cckN* led to hyperactivation of CtrA~P that interfered  
271 with DNA replication initiation and consequently to a reduced viability as estimated by  
272 colony forming units (Figure 4b). The toxicity associated with *cckN* overexpression  
273 was not observed in cells with reduced CtrA activity (*cckATS1* and *ctrA401*) (1, 3) or  
274 abundance (*cpdR<sub>D51A</sub>* and *cpdR<sub>D51A</sub> ΔdivK*) (22) (Figure 4b). Indeed, the  
275 thermosensitive *cckATS1* allele harbours two mutations (I484N and P485A) that  
276 compromise the kinase activity of CckA, thereby decreasing CtrA phosphorylation (3,  
277 30), while the *ctrA401* allele harbours a T170I substitution in CtrA that decreases its  
278 activity (1, 31). On the other hand, CtrA activity is reduced in a *cpdR<sub>D51A</sub>* background  
279 since this phosphoablative variant of CpdR leads to constant degradation of CtrA  
280 along the cell cycle (22). Similarly, CckN variants that are predicted to lack kinase  
281 and phosphatase activities (CckN<sup>K-P-</sup>) – *cckN<sub>H47N</sub>* and *cckN<sub>T51R</sub>*, the latter of which  
282 was designed based on the PleC<sup>K-P-</sup> variant T561R (20) – were less toxic upon  
283 overexpression compared to wild-type CckN (Figure 4c). In contrast, overexpression  
284 of CckN variants predicted to have lost only kinase activity (CckN<sup>K-P+</sup>) – *cckN<sub>F212L</sub>*,  
285 designed based on PleC<sub>F778L</sub> (20), and *cckN<sub>D195N</sub>*, harbouring a mutation in the G1  
286 box required for ATP binding – were still as toxic as the wild-type (Figure 4c). Thus,  
287 our data suggest that the major role of CckN *in vivo* is not to phosphorylate, but to  
288 dephosphorylate DivK and PleD, and thereby to stimulate CtrA activity.

289

290 **Transcription of *cckN* is stimulated by CtrA~P and (p)ppGpp**

291 Since our ChIP-Seq data suggested that *cckN* might be a direct target of CtrA  
292 (Supplementary Table 1), we monitored the activity of  $P_{cckN}$  using a transcriptional  
293 fusion to *lacZ* on a replicative plasmid (pRKlac290- $P_{cckN}$ ) in mutant strains harbouring  
294 higher or lower CtrA activity. We found that the activity of  $P_{cckN}$  was decreased or  
295 increased in strains harbouring lower ( $\Delta pleC$ , *ctrA401* and *cckATS1*) or higher ( $\Delta divJ$   
296 and *divK341*) CtrA activity, respectively (Supplementary Figure 5a, b). These data  
297 suggest that *cckN* is subjected to a positive feedback loop by CtrA~P, but this  
298 regulation might be indirect since we could not identify a predicted consensus CtrA  
299 binding site in the promoter region of *cckN*. We also found that  $P_{cckN}$  activity was  
300 induced upon entry into stationary phase (Supplementary Figure 5c). In agreement  
301 with recent data showing that (p)ppGpp is required to sustain optimal activity of CtrA-  
302 dependent promoters during stationary phase (31), induction of  $P_{cckN}$  was not  
303 observed in (p)ppGpp<sup>0</sup> ( $\Delta spoT$ ) cells (Supplementary Figure 5c). In addition, ectopic  
304 production of (p)ppGpp – by a functional truncated version of the *E. coli* (p)ppGpp  
305 synthetase RelA expressed from the xylose-inducible promoter ( $P_{xyIX}::relA'$ ) at the  
306 *xyIX* locus – increased  $P_{cckN}$  activity in exponentially growing cells only when xylose  
307 was supplemented to the media (Supplementary Figure 5d). In contrast, inducing the  
308 expression of the corresponding catalytically inactive variant of RelA ( $P_{xyIX}::relA'_{E335Q}$ )  
309 with xylose did not change  $P_{cckN}$  activity (Supplementary Figure 5d). Together, these  
310 results suggest that induction of *cckN* expression in stationary phase by CtrA~P is  
311 (p)ppGpp-dependent.

312

### 313 **PleC and CckN are cleared from G1 cells in a ClpXP-dependent way**

314 Based on the results presented above, PleC and CckN protect premature inactivation  
315 of CtrA during the G1 phase of the cell cycle by maintaining the phosphorylation level  
316 of DivK low. At the G1-S transition, DivK~P levels rise to indirectly trigger CtrA  
317 dephosphorylation and ClpXP-dependent proteolysis. This implies that both CckN  
318 and PleC should be inactivated first. Thus, we tested whether CckN abundance  
319 fluctuates along the cell cycle by monitoring levels of CckN fused to a triple FLAG tag  
320 to either its N- or C-terminus expressed as the only copy from the native  
321 chromosomal locus. Interestingly, CckN-3FLAG was present only in G1/swarmer  
322 cells whereas 3FLAG-CckN remained roughly constant throughout the cell cycle  
323 (Figure 5a). The strains expressing a 3FLAG tag at the 5' or 3' extremity of *cckN* did  
324 not display any particular morphological or growth defects in comparison to the wild-

325 type strain. The rapid disappearance of CckN-3FLAG during the G1-S transition  
326 (Supplementary Figure 6a, b) suggests the involvement of ATP-dependent  
327 proteolysis. To identify the protease responsible for CckN proteolysis, CckN-3FLAG  
328 abundance was quantified in a set of known *C. crescentus* protease and proteolytic  
329 adaptors mutant strains. CtrA was used as a control since it is degraded during G1-S  
330 transition by the ClpXP protease with the help of the adaptor proteins CpdR, RcdA  
331 and PopA bound to c-di-GMP (32). As expected, CtrA levels increased in  $\Delta clpX$  and  
332  $\Delta clpP$  strains, as well as in strains lacking its known proteolytic adaptors CpdR, RcdA  
333 and PopA (9, 17, 33) (Figure 5b). Note that deletion of *clpX* and *clpP* genes were in a  
334  $\Delta socAB$  background that suppresses their essentiality (34). CckN-3FLAG levels  
335 increased in the  $\Delta clpX$  and  $\Delta clpP$  mutants, and this effect was independent of ClpXP  
336 proteolytic adaptors required for degradation of cell cycle regulators (Figure 5b) (2,  
337 35-38). In agreement with this result, we found that CckN-3FLAG levels properly  
338 fluctuated throughout the cell cycle in  $\Delta cpdR$  cells, in contrast to CtrA whose  
339 degradation strictly depends on CpdR (Supplementary Figure 6d). As PleC  
340 abundance was also suggested to vary along the cell cycle (39) by disappearing  
341 together with CtrA at the G1-S transition (Supplementary Figure 6a, b), we also  
342 determined PleC abundance in the same protease and proteolytic adaptors mutants.  
343 Similar to CckN, PleC abundance increased in  $\Delta clpX$  and in  $\Delta clpP$  mutants but not in  
344 strains lacking CpdR, RcdA and PopA adaptors (Figure 5b).

345 Previous studies demonstrated that substituting the two C-terminal  
346 hydrophobic residues (AA, AG or VA) of cell cycle regulators proteolyzed by ClpXP  
347 by two aspartate residues (DD) – CtrA<sub>AA::DD</sub>, KidO<sub>VA::DD</sub>, TacA<sub>AG::DD</sub>, GdhZ<sub>AA::DD</sub> and  
348 ShkA<sub>AG::DD</sub> – led to their stabilization (2, 35-38). Since both CckN and PleC displayed  
349 two alanine residues at their C-terminal extremity (Supplementary Figure 6c), we  
350 tested their potential involvement in the recognition of PleC and CckN by ClpX by  
351 creating *pleC*<sub>AA::DD</sub> and *cckN*<sub>AA::DD</sub>-3FLAG mutants and monitoring protein abundance  
352 in asynchronous and synchronized populations. CckN<sub>AA::DD</sub>-3FLAG was not protected  
353 from degradation along cell cycle (Figure 5b, Supplementary Figure 6e) suggesting  
354 that in contrast to most ClpXP substrates, CckN degradation does not rely on a C-  
355 terminal degron. In contrast, PleC<sub>AA::DD</sub> levels increased and did not oscillate  
356 anymore over the cell cycle in comparison to wild-type PleC (Figure 5b,  
357 Supplementary Figure 6f, g), suggesting that the C-terminal motif Ala-Ala is critical

358 for PleC degradation. Given that a 3FLAG fusion at the N-terminal extremity of CckN  
359 led to protein stabilization whereas the same tag at the C-terminal end did not  
360 interfere with proteolysis (Figure 5a), a N-terminal motif instead of the two C-terminal  
361 hydrophobic residues is likely involved in the recognition of CckN by ClpX.  
362 Altogether, our data show that CckN and PleC are degraded in a ClpXP-dependent  
363 manner early in G1 phase, before the inactivation of the master regulator CtrA at the  
364 G1-S transition by dephosphorylation and proteolysis. However, in contrast to cell  
365 cycle regulators described so far to be proteolyzed by ClpXP, including CtrA itself,  
366 degradation of CckN and PleC does not rely on known proteolytic adaptors and  
367 involves – at least for CckN – an unsuspected N-terminal motif. Possibly, yet  
368 unidentified ClpXP adaptor proteins are required for timely degradation of PleC and  
369 CckN at the G1-S transition. Alternatively, PleC and CckN could be directly  
370 recognized by ClpXP without the help of any auxiliary factors.

371

## 372 Discussion

373 CckN was identified almost two decades ago in a yeast two-hybrid screen as a an  
374 interaction partner of the response regulator DivK (13). Here, we confirmed this  
375 interaction and also uncovered CckN as a second functional phosphatase for DivK  
376 and PleD (Figure 1). In contrast to the primary phosphatase PleC whose inactivation  
377 leads to pleiotropic effects, *cckN* loss-of-function mutants ( $\Delta cckN$  or *cckN*<sub>H47A</sub>) did not  
378 display any detectable phenotype in an otherwise wild-type background. In contrast,  
379 deletion of *cckN* in a  $\Delta divJ \Delta pleC$  background led to a decrease of CtrA activity  
380 (Figure 3, Supplementary Figures 1 and 3, Supplementary Table 1) as well as  
381 developmental defects. In addition, a mild overexpression of *cckN* suppresses  $\Delta pleC$   
382 defects associated with its phosphatase, but not kinase, activity (Supplementary  
383 Figure 4), while strong *cckN* overexpression leads to a CtrA-dependent G1 block and  
384 toxicity (Figure 4). Thus, our data suggest that PleC phosphatase might be seconded  
385 by CckN upon specific conditions that still need to be uncovered.

386 Despite the redundancy of their phosphatase activity, CckN and PleC display  
387 different subcellular localization since PleC operates at the swarmer pole while CckN  
388 is diffused into the cytosol (Supplementary Figure 7). It is noteworthy that a CckN-  
389 GFP fusion expressed from the native *cckN* locus was almost undetectable,  
390 suggesting that the expression level of *cckN* is low. It is likely that the polar  
391 localization of PleC (11) has been selected for regulating its kinase rather its  
392 phosphatase activity. Indeed, PleC<sup>K</sup> is allosterically activated at the differentiating  
393 pole by polar DivK~P (15), suggesting that the kinase activity of PleC is restricted to  
394 that pole. On the contrary, DivK~P can still be efficiently dephosphorylated by PleC  
395 without being localized at the pole in  $\Delta spmX$  cells (28). In  $\Delta spmX$ , the activity of the  
396  $\sigma^{54}$ -dependent transcriptional activator TacA is exacerbated (40). A comparative  
397 transposon (Tn) insertions coupled to deep sequencing (Tn-Seq) experiment done on  
398  $\Delta spmX$  vs wild-type cells supported that conclusion, since insertions into genes  
399 coding for positive regulators of TacA activity or expression were over-represented  
400 (40). This was the case for *shkA* coding for the hybrid kinase ShkA activating TacA  
401 by phosphorylation or *rpoN* encoding  $\sigma^{54}$  (40). Interestingly, Tn insertions also  
402 strongly accumulated in *pleC* and *cckN* in this experiment, likely because inactivation  
403 of their phosphatase activity down-regulates the CtrA-dependent  $P_{tacA}$  promoter,  
404 thereby limiting *tacA* expression. Alternatively, or in addition, a reduction in CtrA

405 activity might also result in decreased expression of other genes affecting the ShkA-  
406 TacA pathway, such as *pleD* or other factors that could influence the phosphorylation  
407 state of the PleD/ShkA/TacA axis. Since TacA expression largely relies on the  
408 phosphatase activity of PleC (38), these Tn-Seq data support the redundancy  
409 between CckN and PleC. Notwithstanding, it has been shown that TacA  
410 phosphorylation by ShkA during the G1 phase requires c-di-GMP synthesized by  
411 PleD (38). Since TacA activity – monitored with a  $P_{spmX}::lacZ$  translational fusion –  
412 was not decreased in  $\Delta divJ \Delta pleC$  cells but strongly diminished in  $\Delta pleD$  cells, it has  
413 been proposed that a third histidine kinase phosphorylates PleD in a  $\Delta divJ \Delta pleC$   
414 background (38). In agreement with the fact that CckN does not display kinase  
415 activity (Supplementary Figure 1), we found that  $P_{spmX}$  activity was as high in  
416  $\Delta divJ \Delta pleC \Delta cckN$  cells as in wild-type cells (Supplementary Figure 8), thereby  
417 excluding CckN as the missing kinase for PleD. Thus, other phosphodonors for PleD,  
418 as well as for DivK as already suggested (11), remain to be uncovered. Indeed, the  
419 fact that *cckN* inactivation causes DivK-dependent phenotypes in a  $\Delta divJ \Delta pleC$   
420 background demonstrates that, in the absence of DivJ and PleC, DivK is largely  
421 functional. The fact that CckN does seem to play a modulatory role on DivK/CtrA  
422 activity, rather than an essential, suggests the presence of yet other regulators  
423 affecting DivK.

424 Akin to DivK, PleC and DivJ also modulate PleD phosphorylation (14, 15, 41).  
425 We show here that PleD is completely dephosphorylated *in vivo* upon *cckN*  
426 overexpression (Figure 2e), very likely as a result of two complementary effects.  
427 First, by decreasing phosphorylation levels of DivK, which was shown to allosterically  
428 affect DivJ and PleC kinase activity and thereby PleD phosphorylation (15). Second,  
429 by directly dephosphorylating PleD~P (Figure 2d). Concomitantly maintaining low  
430 PleD~P and DivK~P levels is important for coordinating cell cycle and developmental  
431 control. Indeed, strong activation of PleD in G1 cells would trigger premature  
432 abandon of motility without starting DNA replication. Interestingly, no autokinase  
433 activity was detected with CckN even in the presence  $DivK_{D53N}$ , yet  $DivK_{D53N}$  was  
434 able to strongly induce kinase activity of DivJ and PleC (15) (Supplementary Figure  
435 1).

436 Surprisingly, we observed phosphorylated CckN in the presence of DivJ and  
437 ATP (Supplementary Figure 1c). Thus, CckN and DivJ might interact with each other

438 to form heterodimers in which CckN is trans-phosphorylated by DivJ. If true, this  
439 would even further protect DivK and PleD from premature activation during G1 or G1-  
440 S transition by draining phosphoryl-groups away from DivJ to CckN. CckN could act  
441 as a prototypical phosphatase, *i.e.* catalyzing hydrolysis of phospho-aspartate on  
442 receiver domain (REC-Asp~P) of DivK and PleD via coordination of a water molecule  
443 without being phosphorylated itself. Alternatively, CckN could serve as a sort of  
444 histidine phosphotransferase (Hpt) that accepts phosphoryl groups from REC-Asp~P  
445 in a back-transfer reaction, thereby leading to REC dephosphorylation while being  
446 phosphorylated itself. In fact, the phosphorylatable His residue required for  
447 autophosphorylation is dispensable for phosphatase activity in the prototypical  
448 bifunctional histidine kinase/phosphatase EnvZ, where His243 can be replaced by  
449 several amino acids still allowing significant dephosphorylation of its cognate  
450 substrate, OmpR (42). In contrast, His47 of CckN seems essential for its proposed  
451 function in dephosphorylating DivK and PleD, since replacement of His47 in CckN by  
452 Ala or Asn essentially phenocopies a *cckN* null allele in all assays tested. Of note,  
453 the idea that bifunctional histidine kinases/phosphatases with an intact CA domain  
454 can mainly function as Hpts to distribute phosphoryl groups between up- and  
455 downstream components is not unprecedented. It was recently proposed that LovK  
456 and PhyK involved in the general stress response in *C. crescentus* exert their main  
457 functions by acting as Hpts (43). PhyK and LovK share similarity in their DHP  
458 domains, but belong to different histidine kinase subfamilies, respectively HisKA2  
459 and HWE, the former of which essentially has a CA domain identical to HisKA  
460 kinases with all known residues important for autophosphorylation conserved (43-45).  
461 PhyP from the alphaproteobacterium *Sphingomonas melonis* Fr1 harbours a DHP  
462 domain similar to PhyK/LovK but fails to classify as either HisKA2 or HWE kinase  
463 due to its degenerate CA domain (46). PhyP was initially described as a phosphatase  
464 for PhyR, the response regulator universally controlling the general stress response  
465 in alphaproteobacteria (46, 47). However, PhyP was recently shown to act as a HPT  
466 rather than a true phosphatase, shuttling phosphoryl group towards or away from  
467 PhyR (48). Thus, histidine kinases/phosphatases exist that employ back-transfer of  
468 phosphoryl groups as a means to dephosphorylate response regulator. Whether  
469 CckN (and PleC) belong to this group of enzymes employing such a mechanism  
470 remains to be studied in the future.

471 Our data strongly suggest that both CckN and PleC are proteolyzed in a  
472 ClpXP-dependent manner in early G1 cells (Figure 5, Supplementary Figure 6).  
473 Unexpectedly and in contrast to any ClpXP substrates described to date, it seems  
474 that none of the known proteolysis adaptors is required for CckN or PleC  
475 degradation. This is surprising knowing that CckN was found as a potential partner of  
476 RcdA in a pull-down assay (49). RcdA is proteolytic adaptor that delivers some ClpXP  
477 substrates (e.g. TacA) to the CpdR-primed ClpXP protease (49). Thus, it is possible  
478 that CckN interacts with RcdA to limit its availability as a protease adaptor during  
479 early G1 phase, thereby avoiding premature RcdA functions in the hierarchical  
480 proteolytic events. Although we cannot exclude the possibility that PleC and CckN  
481 are directly recognized and bound by ClpX to be degraded, their rapid turnover in G1  
482 phase suggests the existence of a novel adaptor protein primed to ClpXP.

483 Since CckN is restricted to G1 cells in *C. crescentus*, its functions could be  
484 required in conditions leading to an extended G1 phase. In its natural oligotrophic  
485 environment, *C. crescentus* is expected to encounter extended periods of nutrient  
486 starvation during which the swarmer cells might not initiate DNA replication. Indeed,  
487 we know that limiting nitrogen or carbon leads to a (p)ppGpp-dependent G1 block in  
488 *C. crescentus* (50, 51) and that *cckN* expression is positively regulated by (p)ppGpp  
489 (Supplementary Figure 5c, d). In these stressful conditions, CckN might therefore be  
490 required to second PleC in maintaining DivK phosphorylation low and avoiding  
491 premature inactivation CtrA~P. We tested this hypothesis by comparing the viability  
492 of wild-type and  $\Delta cckN$  cells maintained in stationary phase of growth. However,  
493 despite a (p)ppGpp-dependent induction of *cckN* expression in these conditions,  
494  $\Delta cckN$  cells remained as viable as the wild-type when maintained in stationary phase  
495 for days (Supplementary Figure 5e). Likewise, we did not find any particular stressful  
496 conditions (nutrient starvation, oxidative stress, heavy metal exposure, temperatures,  
497 ...) that decreased viability of  $\Delta cckN$  more than wild-type cells, whether *pleC* was  
498 present or not, and whether the strains were incubated individually or mixed equally  
499 in the same culture (data not shown). However, the laboratory conditions in which we  
500 measured the fitness cost of *cckN* inactivation remain far from the natural habitats.

501 In alphaproteobacteria, DivK phosphorylation is known to be regulated by  
502 multiple paralogous histidine kinases, which based on similarity of their DHP domains  
503 belongs to the PleC/DivJ-like family, with numbers ranging from one in the obligate

504 intracellular pathogen *Rickettsia prowazekii* to four in the facultative host-associated  
505 bacteria *Sinorhizobium meliloti* or *Agrobacterium tumefaciens* (52-58). Interestingly,  
506 the role played by these proteins on DivK phosphorylation varies between species.  
507 For instance, *B. abortus* PdhS is a *bona fide* bi-functional HK regulating positively  
508 and negatively the phosphorylation of DivK (59). In contrast, neither DivJ nor PleC  
509 was able to modulate DivK phosphorylation (Nayla Francis, personal communication)  
510 or localization (53). However, as both HK can physically interact with DivK, it has  
511 been hypothesized that DivJ and PleC could display kinase or phosphatase activity in  
512 specific conditions, such as in *Brucella*-containing vacuoles during cellular infection.  
513 In *S. meliloti*, DivK can be phosphorylated by DivJ and CbrA and dephosphorylated  
514 by PleC (56), whereas the function of PdhSA remains unknown. Thus, the multiple  
515 PleC/DivJ-like proteins that interact with DivK likely refer to the various environments  
516 encountered by these alphaproteobacteria depending on their lifestyles. The  
517 challenge now will be to identify the specific stimuli regulating the activity of these  
518 DivK-associated HK.

519

## 520 **Material & Methods**

### 521 **Bacterial strains and growth conditions**

522 *Escherichia coli* Top10 was used for cloning purpose, and grown aerobically in Luria-  
523 Bertani (LB) broth (Sigma). Electrocompetent or thermos-competent cells were used  
524 for transformation of *E. coli*. All *Caulobacter crescentus* strains used in this study are  
525 derived from the synchronizable wild-type strain NA1000, and were grown at 30 °C in  
526 Peptone Yeast Extract (PYE) or synthetic media supplemented with glucose (M2G or  
527 M5G) as already described in (51). Genes expressed from the inducible *xyIX*  
528 promoter ( $P_{xyIX}$ ) was induced with 0.1% to 0.2% xylose in *xyIX*<sup>+</sup> background. Motility  
529 was assayed on PYE plates containing 0.3% agar. Generalized transduction was  
530 performed with phage Cr30 according to the procedure described in (60).

531 For *E. coli*, antibiotics were used at the following concentrations (µg/ml; in liquid/solid  
532 medium): ampicillin (100/100), kanamycin (30/50), oxytetracycline (12.5/12.5),  
533 spectinomycin (100/100), streptomycin (50/100) or chloramphenicol (20/30) For *C.*  
534 *crescentus*, media were supplemented with kanamycin (5/20), oxytetracycline  
535 (2.5/2.5), spectinomycin (25/50), streptomycin (5/5), hygromycin (100/100), nalidixic  
536 acid (20), chloramphenicol (1/2) or gentamycin (0.5/5) when appropriate. Cumate (4-  
537 isopropylbenzoic acid) was dissolved in 100% ethanol to result in a 1000X 100 mM  
538 stock solution and used at a final concentration of 100 µM in plates. For “no cumate”  
539 controls, an equal volume of ethanol was added to plates.

540

541 **Motility assay.** Five microliters of saturated overnight cultures was inoculated into  
542 PYE 0.3% swarm agar plates and the plates were incubated at 30° C for 3-5 days.  
543 ImageJ software was then used to quantify areas of the swarm colonies as described  
544 previously in (51).

545

### 546 **Bacteriophage sensitivity assays**

547 The sensitivity to CbK (LHR1) and CR30 (LHR2) bacteriophages were performed as  
548 follows. First, 200 µl overnight culture of *Caulobacter* cells grown in PYE were mixed  
549 to 4-5 ml of prewarmed PYE Top Agar (0.45% agar) medium and poured on a PYE  
550 plain agar plate. Then, CbK and Cr30 bacteriophage lysates were serially diluted  
551 spotted (5 µl drops) on the Top Agar once solidified and incubated overnight at 30 °C.

552

553 **Construction of plasmids and strains**

554 Detailed descriptions of bacterial strains are included in the Supplementary  
555 Information. Strains, plasmids and oligonucleotides used for plasmids and strains  
556 construction are listed in Tables S2-S4. *E. coli* S17-1 and *E. coli* MT607 helper  
557 strains were used for transferring plasmids to *C. crescentus* by respectively bi- and  
558 tri-parental matings. In-frame deletions were created by using the pNPTS138-  
559 derivative plasmids as follows. Integration of the plasmids in the *C. crescentus*  
560 genome after single homologous recombination were selected on PYE plates  
561 supplemented with kanamycin. Three independent recombinant clones were  
562 inoculated in PYE medium without kanamycin and incubated overnight at 30 °C.  
563 Then, dilutions were spread on PYE plates supplemented with 3% sucrose and  
564 incubated at 30 °C. Single colonies were picked and transferred onto PYE plates with  
565 and without kanamycin. Finally, to discriminate between mutated and wild-type loci,  
566 kanamycin-sensitive clones were tested by PCR on colony using locus-specific  
567 oligonucleotides.

568

569 **Attachment assays**

570 Overnight cultures were diluted in a 96-well microplate and incubated for 18 h to 24 h  
571 at 30 °C before measuring absorbance at the optical density of 660 nm (OD<sub>660</sub>).  
572 Unattached cells were discarded and the microplate was washed 3 times with dH<sub>2</sub>O.  
573 Then, 0.1% crystal Violet (CV) was added for 15 min under agitation before washing  
574 the wells with dH<sub>2</sub>O. Finally, CV was dissolved in a 20% acetic acid solution for 15  
575 min under agitation and absorbance at 595 nm (OD<sub>595</sub>) was taken. To normalize  
576 attachment to growth, the ratio between OD<sub>595</sub> and OD<sub>660</sub> was used.

577

578 **Spotting assays**

579 For experiments shown in Figure 4b, c, 10-fold serial dilutions (in PYE) were  
580 prepared in 96-well plates from 5 ml cultures in standard glass tubes grown overnight  
581 at 30 °C in PYE Kan (Figure 4b) or Tet (Figure 4c) and dilution series were spotted  
582 on PYE Kan and PYE Kan 0.1% xylose (Figure 4b) or replica-spotted on PYE Tet  
583 and PYE Tet Q100 plates using an in-house-made 8-by-6 (48-well) metal pin  
584 replicator (Figure 4c). Plates were incubated at 30 °C for two days and pictures were  
585 taken.

586

587 **Synchronization of cells**

588 Synchronization of cells was performed as already described in (37). Briefly, cells  
589 were grown in 200 ml of PYE to OD<sub>660</sub> of 0.6, harvested by centrifugation for 20 min  
590 at 5,000 x g, 4 °C; resuspended in 60 ml of ice-cold Phosphate (PO<sub>4</sub><sup>3-</sup>) buffer and  
591 combined with 30 ml of Ludox LS Colloidal Silica (30%) (Sigma-Aldrich). Cells  
592 resuspended in Ludox was centrifuged for 40 min at 9,000 x g, 4 °C. Swarmer cells,  
593 corresponding to the bottom band, were isolated, washed twice in ice-cold PO<sub>4</sub><sup>3-</sup>  
594 buffer, and finally resuspended in prewarmed PYE media for growth at 30 °C.  
595 Samples were collected every 15 min for western blot, microscopy and FACS  
596 analyses.

597

598 **Proteins purification**

599 In order to immunize rabbits for production of polyclonal antibodies and or to perform  
600 *in vitro* phosphorylation assays, DivJ<sup>Sm</sup>, CckN, DivK and His6-PleC<sub>505-842</sub> was purified  
601 as follows. A BL21 (DE3) strain harbouring plasmid pML31-TRX-His6-*divJ*<sup>HK<sub>Sm</sub></sup> (56),  
602 pET-28a-*cckN*, pET-28a-*divK* or pET-28a-*pleC*<sub>505-842</sub> was grown in LB medium  
603 supplemented with kanamycin until OD<sub>600</sub> of 0.7. IPTG was added at a final  
604 concentration of 1 mM and the culture was incubated at 37 °C for 4 h. Then, cells  
605 were harvested by centrifugation for 20 min at 5,000 x g, 4 °C. The pellet was  
606 resuspended in 20 ml BD buffer (20 mM Tris-HCl pH 8.0, 500 mM NaCl, 10%  
607 glycerol, 10 mM MgCl<sub>2</sub>, 12.5 mM Imidazole) supplemented with complete EDTA-free  
608 protease cocktail inhibitor (Roche), 400 mg lysozyme (Sigma) and 10 mg DNaseI  
609 (Roche) and incubated for 30 min on ice. Cells were then lysed by sonication and the  
610 lysate by centrifugation 12,000 rpm for 30 min at 4°C was loaded on a Ni-NTA  
611 column and incubated 1 h at 4 °C with end-over-end shaking. The column was then  
612 washed with 5 ml BD buffer, 3 ml Wash1 buffer (BD buffer with 25 mM imidazole), 3  
613 ml Wash2 buffer (BD buffer with 50 mM imidazole), 3 ml Wash3 buffer (BD buffer  
614 with 75 mM imidazole). Proteins bound to the column were eluted with 3 ml Elution  
615 buffer (BD buffer with 100 mM imidazole) and aliquoted in 300 µl fractions. All the  
616 fractions containing the protein of interest (checked by Coomassie blue staining)  
617 were pooled and dialyzed in Dialysis buffer (50 mM Tris pH 7.4, 12.5 mM MgCl<sub>2</sub>).  
618 For experiments shown in Figure 2d and Supplementary Figure 1, proteins were  
619 expressed in *E. coli* BL21 (DE3) harbouring plasmid pETHisMBP-*cckN*, pETHisMBP-  
620 *divJ* or pETHisMBP-*pleC*, or in *E. coli* BL21 (DE3) pLys harbouring plasmids pCC2 or

621 pRP112. Strains were grown overnight in 5 ml LB-Miller at 37 °C with appropriate  
622 antibiotics, diluted 100-fold in 500 ml LB-Miller with appropriate antibiotics and grown  
623 at 37 °C until the cultures reached an OD<sub>600</sub> of 0.5–0.8. Cultures were then shifted to  
624 23 °C and incubated for another hour, after which protein expression was induced by  
625 addition of 0.2 mM IPTG. After incubation overnight, cells were harvested by  
626 centrifugation (5000 × g, 20 min, 4 °C), washed once with 20 ml of 1X PBS, flash-  
627 frozen in liquid N<sub>2</sub> and stored at –80 °C until purification. For purification, the pellet  
628 was resuspended in 8 ml of buffer A (2X PBS containing 500 mM NaCl, 10 mM  
629 imidazole and 2 mM β-mercaptoethanol) supplemented with DNaseI (AppliChem)  
630 and Complete Protease inhibitor (Roche). After one passage through a French press  
631 cell, the suspension was centrifuged (10,000 × g, 30 min, 4 °C) and the supernatant  
632 was mixed with 800 μl of Ni-NTA slurry, prewashed with buffer A, and incubated for  
633 1-2 h on a rotary wheel at 4 °C. Ni-NTA agarose was loaded on a polypropylene  
634 column and washed with at least 50 ml of buffer A, after which the protein was eluted  
635 with 2.5 ml of buffer A containing 500 mM imidazole. The eluate was immediately  
636 loaded on a PD-10 column pre-equilibrated with kinase buffer (10 mM HEPES-KOH  
637 pH 8.0, 50 mM KCl, 10% glycerol, 0.1 mM EDTA, 5 mM MgCl<sub>2</sub>, 5 mM β-  
638 mercaptoethanol). The protein was then eluted with 3.5 ml of kinase buffer and  
639 stored at 4 °C until further use. All experiments were performed within one week after  
640 purification.

641

#### 642 **Immunoblot analysis**

643 Proteins crude extracts were prepared by harvesting cells from exponential growth  
644 phase (OD<sub>660</sub> ~0.3). The pellets were then resuspended in SDS-PAGE loading buffer  
645 by normalizing to the OD<sub>660</sub> before lysing cells by incubating them for 10 min at 95 °C.  
646 The equivalent of 0.5 ml of cult (OD<sub>660</sub> = 0.3) was loaded and proteins were  
647 subjected to electrophoresis in a 12% SDS-polyacrylamide gel, transferred onto a  
648 nitrocellulose membrane then blocked overnight in 5% (wt/vol) nonfat dry milk in  
649 phosphate buffer saline (PBS) with 0.05% Tween 20. Membrane was immunoblotted  
650 for ≥ 3 h with primary antibodies : anti-M2 (1:5,000) (Sigma), anti-CtrA (1:5,000), anti-  
651 MreB (1:5,000), anti-PleC (1:5,000), anti-CckN (1:2,000), anti-DivK (1:2,000) then  
652 followed by immunoblotting for ≤ 1 h with secondary antibodies: 1:5,000 anti-mouse  
653 (for anti-FLAG) or 1:5000 anti-rabbit (for all the others) linked to peroxidase (Dako

654 Agilent), and visualized thanks to Clarity™ Western ECL substrate  
655 chemiluminescence reagent (BioRad) and Amersham Imager 600 (GE Healthcare).

656

### 657 **FACS analysis**

658 Bacterial cells were incubated at 30 °C until they reached mid-log phase, and 100 µL  
659 cells was added to 900 µl ice-cold 70% (vol/vol) ethanol solution and stored at -20 °C  
660 for 4 h or until further use. For rifampicin treatment, the mid-log phase cells were  
661 grown in the presence of 20 µg/mL rifampicin at 30 °C for 3 h. One milliliter of these  
662 cells was fixed as mentioned above. For staining and analysis, 2 ml fixed cells were  
663 pelletized and washed once with 1 ml staining buffer (10 mM Tris-HCl pH 7.2, 1 mM  
664 EDTA, 50 mM sodium citrate + 0.01% TritonX-100). Then, cells were resuspended in  
665 1 ml staining buffer containing 0.1 mg/ml RNaseA (Roche Life Sciences) and  
666 incubated at room temperature (RT) for 30 min. The cells were then harvested by  
667 centrifugation at 6,000 × g for 2 min, and the pellets were resuspended in 1 ml  
668 staining buffer supplemented with 0.5 µM Sytox Green Nucleic Acid Stain (Molecular  
669 Probes, Life Technologies), followed by incubation in the dark for 5 min. These cells  
670 were then analyzed immediately in flow cytometer (FACS Calibur, BD Biosciences)  
671 at laser excitation of 488 nm. At least 1 × 10<sup>4</sup> cells were recorded in triplicate for each  
672 experiment.

673

### 674 **Microscopy**

675 All strains were imaged during exponential phase of growth (OD<sub>660</sub> between 0.1 and  
676 0.4) after immobilization on 1.5% PYE agarose pads. Microscopy was performed  
677 using Axioskop microscope (Zeiss), Orca-Flash 4.0 camera (Hamamatsu) and Zen  
678 2.3 software (Zeiss). Images were processed using ImageJ.

679

### 680 ***In vivo* <sup>32</sup>P labelling**

681 A single colony of cells picked from a PYE agar plate was washed with M5G medium  
682 lacking phosphate and was grown overnight in M5G with 0.05 mM phosphate to  
683 OD<sub>660</sub> of 0.3. Then, one milliliter of culture was harvested and resuspended in the  
684 same volume of SDS-PAGE loading buffer to determine the relative protein content  
685 by immunoblot, and one milliliter of culture was labelled for 4 min at 30 °C using 30  
686 µCi γ-[<sup>32</sup>P]ATP. Following lysis, proteins were immunoprecipitated with 3 µl of

687 polyclonal anti-sera (anti-CtrA or anti-PleD). The precipitates proteins were resolved  
688 by SDS-PAGE and [<sup>32</sup>P]-labelled proteins was visualized using a Super Resolution  
689 screen (Perkin Elmer and quantified using a Cyclone Plus Storage Phosphor System  
690 (Perkin Elmer). The signal was normalized to the relative protein content determined  
691 by immunoblotting of whole cell lysates probed with antibodies. Note that we checked  
692 on cold samples that immunoprecipitation of CtrA or PleD was comparable from one  
693 strain to the other.

694

### 695 ***In vitro* phosphorylation assays**

696 For experiments shown in Figure 2c, autophosphorylation was performed on 5 μM of  
697 DivJ<sub>Sm</sub> kinase in 50 mM Tris-HCl pH 7.4 supplemented with 2 mM DTT, 5 mM MgCl<sub>2</sub>,  
698 500 μM ATP and 2 μCi γ-[<sup>32</sup>P]ATP at 30°C for 40 min. Then, 5 μM of DivK were  
699 added to the mix supplemented with 5 mM MgCl<sub>2</sub> and phosphotransfer was  
700 performed at RT for 15 min. To remove excess of ATP, sample was washed twice in  
701 amicon column with a cut-off of 10 KDa by adding 450 μl of 50 mM Tris-HCl pH 7.4  
702 and centrifuging 10 min at 12,000 rpm. CckN was then added at a final concentration  
703 of 5 μM and the mix was incubated 1, 2 and 5 min at RT. Reaction was stopped by  
704 adding SDS-PAGE loading buffer and samples were resolved by SDS-PAGE, the  
705 dried gel was visualized using a Super Resolution screen (Perkin Elmer) and  
706 quantified using a Cyclone Plus Storage Phosphor System (Perkin Elmer).

707 For experiments shown in Figure 2d and Supplementary Figure 1, all reactions were  
708 performed in kinase buffer supplemented with 433 μM ATP and 5-20 μCi γ-[<sup>32</sup>P]ATP  
709 (3000 Ci/mmol, Hartmann Analytic) at room temperature. For experiments shown in  
710 Supplementary Figure 1a, reactions containing His6-MBP-PleC (5 μM), His6-MBP-  
711 DivJ (5 μM) or His6-MBP-CckN (5 μM) without or with DivK<sub>D53N</sub> (10 μM) were  
712 prepared and incubated for 20 min at RT before autophosphorylation was started by  
713 addition of ATP. Aliquots were withdrawn from the reactions as indicated in the figure  
714 and stopped by addition of 5X SDS sample buffer and stored on ice. For experiments  
715 shown in Supplementary Figure 2b, reactions containing His6-MBP-DivJ (9 μM),  
716 His6-MBP-CckN (11 μM), PleD (28 μM) and/or DivK<sub>D53N</sub> (28 μM) were prepared and  
717 incubated for 30 min at RT before autophosphorylation was started. Reactions were  
718 stopped after 60 min by addition of 5X SDS sample buffer and stored on ice. For  
719 reactions shown in Figure 2d, His-MBP-DivJ (10 μM) was autophosphorylated for 60

720 min in a reaction volume of 150  $\mu$ l, then 20  $\mu$ L of PleD (8  $\mu$ M final) were added, the  
721 reaction was split in 40  $\mu$ l aliquots and, after allowing PleD phosphorylation for 2 min,  
722 10  $\mu$ l of His6-MBP-CckN (4  $\mu$ M final) or kinase buffer (control) were added. Aliquots  
723 were withdrawn from the reactions as indicated in the figure and stopped by addition  
724 of 5X SDS sample buffer and stored on ice. Reactions were run on precast Mini-  
725 Protean TGX (Biorad) gels, wet gels were exposed to a phosphor screen, which was  
726 subsequently scanned using a Typhoon FLA 7000 imaging system (GE Healthcare).

727

### 728 **Quantification of DivJ and PleC phosphorylation**

729 For quantification of DivJ and PleC phosphorylation *in vitro*, the upper bands in gels  
730 shown in Supplementary Figure 1a corresponding to full-length MBP-DivJ and MBP-  
731 PleC were subjected to measurements (“integrated density”) with a “rectangle” of  
732 fixed size using FIJI. For each gel, a “rectangle” of the same size left to lane 1 (a part  
733 of the gel that had no proteins/sample loaded) was used to measure the background,  
734 the value of which was subtracted from all other measured band intensities to obtain  
735 “background-corrected” absolute values. Values were normalized to the signal  
736 obtained after 60 min autophosphorylation of DivJ or PleC without DivK<sub>D53N</sub>  
737 (expressed in % in Supplementary Figure 1b). Note that reactions with and without  
738 DivK<sub>D53N</sub> for DivJ or PleC were run on the same gel to ensure proper comparison of  
739 results with and without DivK<sub>D53N</sub>.

740

### 741 **$\beta$ -galactosidase assays**

742 Overnight saturated cultures of *Caulobacter* cells harbouring lacZ reporter plasmids  
743 were diluted  $\geq 50$ X in fresh medium and incubated at 30  $^{\circ}$ C until OD<sub>660</sub> of 0.3 to 0.5.  
744 For  $\beta$ -galactosidase assays done in stationary phase (Supplementary Figure 5b),  
745 cells were incubated at 30  $^{\circ}$ C for 24 hrs (final OD<sub>660</sub>~1.3). Fifty microliters aliquots of  
746 the cells were treated with few drops of chloroform. To this, 750  $\mu$ l of Z buffer (60 mM  
747 Na<sub>2</sub>HPO<sub>4</sub>, 40 mM NaH<sub>2</sub>PO<sub>4</sub>, 10 mM KCl, 1 mM MgSO<sub>4</sub>, pH 7.0) was added, followed  
748 by 200  $\mu$ l of 4 mg/ml O-nitrophenyl- $\beta$ -D-galactopyranoside (ONPG). Then, reaction  
749 was incubated at 30  $^{\circ}$ C until yellow color was developed, stopped by addition of 500  
750  $\mu$ l of 1 M Na<sub>2</sub>CO<sub>3</sub> and OD<sub>420</sub> of the supernatant was measured. The activity of the  $\beta$ -  
751 galactosidase expressed in miller units (MU) was calculated using the following  
752 equation:  $MU = (OD_{420} \times 1,000) / [OD_{660} \times t \times v]$  where “t” is the time of the reaction

753 (min), and “v” is the volume of cultures used in the assays (ml). Experimental values  
754 were the average of three independent experiments.

755

#### 756 **Bacterial two-hybrid (BTH) assays**

757 BTH assays were performed as described previously in (51). Briefly, 2  $\mu$ l of MG1655  
758 *cyaA::frt* (RH785) strains expressing T18 and T25 fusions were spotted on  
759 MacConkey Agar Base plates supplemented with ampicillin, kanamycin, maltose  
760 (1%) and IPTG (1 mM), and incubated for 3-4 days at 30 °C. All proteins were fused  
761 to T25 at their N-terminal extremity (pKT25) or to the T18 at their N- (pUT18C) or C-  
762 terminal (pUT18) extremity. The  $\beta$ -galactosidase assays were performed on 50  $\mu$ l *E.*  
763 *coli* BTH strains cultivated overnight at 30° C in LB medium supplemented with  
764 kanamycin, ampicillin and IPTG (1 mM) as described in (61).

765

#### 766 **Co-immunoprecipitation (Co-IP) assays**

767 *C. crescentus* cells were grown in 200 ml of PYE (supplemented with 0.1% xylose if  
768 required) to OD<sub>660</sub> of 0.7 to 0.9, harvested by centrifugation for 20 min at 5,000 x g,  
769 4°C. The pellets were washed once with PBS and resuspended in 10 ml PBS  
770 containing 2 mM DTSP (Dithiobis(succinimidyl propionate)) for crosslinking. After 30  
771 min at 30°C, cross-linking was quenched by the addition of Tris-HCl to a final  
772 concentration of 0.150 M for 30 minutes. Cells were then washed twice with PBS and  
773 once with 20 ml Co-IP buffer (20 mM HEPES, 150 mM NaCl, 20% glycerol, 80 mM  
774 EDTA). The pellets were resuspended in lysis buffer [1x CellLytic B (Sigma), 10 mM  
775 MgCl<sub>2</sub>, 67.5U Ready-Lyse lysozyme (Epicentre), 10U/mL DNase I, 2% NP-40  
776 Surfact-Amps Detergent (Thermo Scientific), ½ tablet Complete EDTA-free anti-  
777 proteases (Roche)] and incubated under soft agitation at RT for 30 min. Cells were  
778 then lysed by sonication, lysates were cleared by centrifugation and incubated 2 h at  
779 4 °C with MagStrep type3 XT beads (Iba). The beads were washed 6 times with W  
780 Buffer (Iba) and precipitated proteins were released by 15 min incubation in BX  
781 Buffer (Iba). SDS loading buffer was added to samples and boiled for 10 min. Equal  
782 volumes of coimmunoprecipitates, and cell lysates from equal numbers of cells, were  
783 analyzed by SDS-PAGE and Western blotting. Membranes were probed with anti-  
784 DivK and anti-CckN primary antibodies.

785

#### 786 **Chromatin immunoprecipitation followed by deep sequencing (ChIP-Seq)**

787 **assays**

788 ChIP-Seq assays were performed as described previously in (62). Briefly, 80 ml of  
789 mid-log phase cells ( $OD_{660}$  of 0.6) were cross-linked in 1% formaldehyde and 10 mM  
790 sodium phosphate (pH 7.6) at room temperature for 10 min and 30 min on ice  
791 thereafter. Crosslinking was stopped by addition of 125 mM glycine and incubated for  
792 5 min on ice. Cells were washed thrice in PBS, resuspended in 450  $\mu$ l in TES buffer  
793 (10 mM Tris-HCl pH 7.5, 1 mM EDTA, 100 mM NaCl) and lysed with 2  $\mu$ l of Ready-  
794 lyse lysozyme solution for 5 min at RT. Protease inhibitors (Roche) was added and  
795 incubated for 10 min. Then, 550  $\mu$ l of ChIP buffer (1.1% triton X-100, 1.2 mM EDTA,  
796 16.7 mM Tris-HCl pH 8.1, 167 mM NaCl, plus protease inhibitors) was added to the  
797 lysate and incubated at 37 °C for 10 min before sonication (2 x 8 bursts of 30 sec on  
798 ice using a Diagenode Bioruptor) to shear DNA fragments to a length of 300 to 500  
799 bp. Lysate was cleared by centrifugation for 10 min at 12,500 rpm at 4 °C and protein  
800 content was evaluated by measuring  $OD_{280}$ . Then, 7.5 mg of proteins were diluted in  
801 ChIP buffer supplemented with 0.01% SDS and precleared 1 h at 4 °C with 50  $\mu$ l of  
802 protein A agarose beads (BioRad) and 100  $\mu$ g BSA. Two  $\mu$ l of polyclonal anti-CtrA  
803 antibodies were added to the supernatant before overnight incubation at 4 °C under  
804 gentle agitation. Eighty  $\mu$ l of BSA pre-saturated protein A agarose beads were added  
805 to the solution for 2 h at 4 °C with rotation, washed once with low salt buffer (0.1%  
806 SDS, 1% Triton X-100, 2 mM EDTA, 20 mM Tris-HCl pH 8.1, 150 mM NaCl), once  
807 with high salt buffer (0.1% SDS, 1% Triton X-100, 2 mM EDTA, 20 mM Tris-HCl pH  
808 8.1, 500 mM NaCl), once with LiCl buffer (0.25 M LiCl, 1% NP-40, 1% deoxycholate,  
809 1 mM EDTA, 10 mM Tris-HCl pH 8.1), once with TE buffer (10 mM Tris-HCl pH 8.1, 1  
810 mM EDTA) at 4 °C and a second wash with TE buffer at RT. The DNA-protein  
811 complexes were eluted twice in 250  $\mu$ l freshly prepared elution buffer (0.1 M  
812  $NaHCO_3$ , 1% SDS). NaCl was added at a concentration of 300 mM to the combined  
813 eluates (500  $\mu$ l) before overnight incubation at 65 °C to reverse the crosslink. The  
814 samples were treated with 20  $\mu$ g of proteinase K in 40 mM EDTA and 40 mM Tris-  
815 HCl (pH 6.5) for 2 h at 45 °C. DNA was extracted using Nucleospin PCR clean-up kit  
816 (Macherey-Nagel) and resuspended in 50  $\mu$ l elution buffer (5 mM Tris-HCl pH 8.5).  
817 DNA sequencing was performed using Illumina HiSeq4000 (Genomicscore  
818 KULeuven, Belgium).

819

820 **NGS data analysis**

821 Around  $2 \times 10^7$  single-end sequence reads (1 x 50) were first mapped on the genome  
822 of *C. crescentus* NA1000 (NC\_011916.1) and converted to SAM using BWA (63) and  
823 SAM (64) tools respectively from the sourceforge server (<https://sourceforge.net/>).  
824 MACS2 (65) algorithm was used to model the length of DNA fragment as well as the  
825 shift size. Next, the number of reads overlapping each genomic position was  
826 computed using custom Python scripts and the previously modelled DNA fragment  
827 and shift sizes. A peak was defined as the genomic region where each position has  
828 more reads than the 97<sup>th</sup> percentile. The candidate peaks were annotated using  
829 custom Python scripts. In the purpose to compare strains, the total number of reads  
830 was normalized by the ratio of the number of reads between the two strains.

831

832 **Statistical analyses.** The significance of differences between mean values was  
833 determined by one-way or two-way ANNOVA with a Tukey's, Dunnett's or Sidak's  
834 multiple comparisons post-test. All the analyses were performed using GraphPad  
835 Prism 8 software. A *P* value of <0.05 was considered as significant.

836

837 **Data availability**

838 ChIP-Seq data have been deposited to the Gene Expression Omnibus (GEO)  
839 database with the accession number GSE152025.

840 **Acknowledgements**

841 We are grateful to Patrick Viollier and Peter Chien for providing strains and plasmids;  
842 Emanuele Biondi for anti-CtrA antibodies; Fanny Zola and Aurélie Mayard for help  
843 with proteins purification. We thank the members of the BCcD team for critical  
844 reading of the manuscript and helpful discussions. The work conducted in the  
845 laboratory of U.J. was supported by the Swiss National Science Foundation (grants  
846 31003A\_166503 and 310030B\_185372). This work was supported by a Research  
847 Credit (CDR J.0169.16) and Incentive Grant for Scientific Research (MIS F.4516.19)  
848 from the Fonds de la Recherche Scientifique – FNRS (F.R.S. – FNRS) to R.H. and  
849 R.H. is a Research Associate of F.R.S. – FNRS.

850

851 **Author Contributions**

852 J.C., A.K., U.J. and R.H. conceived and designed the experiments. J.C. performed all  
853 the experiments except otherwise stated. A.K. performed *in vitro* phosphorylation  
854 assays shown in Figure 2d and Supplementary Figure 1 as well as the growth assays  
855 upon overexpression of *cckN* variants shown in Figure 4c. K.P. designed the  
856 bioinformatic tool to analyse the ChIP-Seq data. T.B. characterized the ClpXP-  
857 dependent degradation of PleC (Figure 5b, c and Supplementary Figure 6f, g). J.C.,  
858 A.K., U.J. and R.H. analyzed the data. J.C., A.K. and R.H wrote the paper.

859

860 **Competing financial interests**

861 The authors declare no competing financial interests.

862

863 **References**

- 864 1. Quon KC, Marczyński GT, Shapiro L. 1996. Cell cycle control by an essential  
865 bacterial two-component signal transduction protein. *Cell* 84:83-93.
- 866 2. Domian IJ, Quon KC, Shapiro L. 1997. Cell type-specific phosphorylation and  
867 proteolysis of a transcriptional regulator controls the G1-to-S transition in a  
868 bacterial cell cycle. *Cell* 90:415-24.
- 869 3. Jacobs C, Domian IJ, Maddock JR, Shapiro L. 1999. Cell cycle-dependent  
870 polar localization of an essential bacterial histidine kinase that controls DNA  
871 replication and cell division. *Cell* 97:111-20.
- 872 4. Biondi EG, Reisinger SJ, Skerker JM, Arif M, Perchuk BS, Ryan KR, Laub MT.  
873 2006. Regulation of the bacterial cell cycle by an integrated genetic circuit.  
874 *Nature* 444:899-904.
- 875 5. Wu J, Ohta N, Zhao JL, Newton A. 1999. A novel bacterial tyrosine kinase  
876 essential for cell division and differentiation. *Proc Natl Acad Sci U S A*  
877 96:13068-73.
- 878 6. Reisinger SJ, Huntwork S, Viollier PH, Ryan KR. 2007. DivL performs critical  
879 cell cycle functions in *Caulobacter crescentus* independent of kinase activity. *J*  
880 *Bacteriol* 189:8308-20.
- 881 7. Iniesta AA, Hillson NJ, Shapiro L. 2010. Cell pole-specific activation of a  
882 critical bacterial cell cycle kinase. *Proc Natl Acad Sci U S A* 107:7012-7.
- 883 8. Childers WS, Xu Q, Mann TH, Mathews, II, Blair JA, Deacon AM, Shapiro L.  
884 2014. Cell fate regulation governed by a repurposed bacterial histidine kinase.  
885 *PLoS Biol* 12:e1001979.
- 886 9. Iniesta AA, McGrath PT, Reisenauer A, McAdams HH, Shapiro L. 2006. A  
887 phospho-signaling pathway controls the localization and activity of a protease  
888 complex critical for bacterial cell cycle progression. *Proc Natl Acad Sci U S A*  
889 103:10935-40.
- 890 10. Laub MT, Chen SL, Shapiro L, McAdams HH. 2002. Genes directly controlled  
891 by CtrA, a master regulator of the *Caulobacter* cell cycle. *Proc Natl Acad Sci U*  
892 *S A* 99:4632-7.
- 893 11. Wheeler RT, Shapiro L. 1999. Differential localization of two histidine kinases  
894 controlling bacterial cell differentiation. *Mol Cell* 4:683-94.
- 895 12. Jacobs C, Hung D, Shapiro L. 2001. Dynamic localization of a cytoplasmic  
896 signal transduction response regulator controls morphogenesis during the  
897 *Caulobacter* cell cycle. *Proc Natl Acad Sci U S A* 98:4095-100.
- 898 13. Ohta N, Newton A. 2003. The core dimerization domains of histidine kinases  
899 contain recognition specificity for the cognate response regulator. *J Bacteriol*  
900 185:4424-31.
- 901 14. Aldridge P, Paul R, Goymer P, Rainey P, Jenal U. 2003. Role of the GGDEF  
902 regulator PleD in polar development of *Caulobacter crescentus*. *Mol Microbiol*  
903 47:1695-708.
- 904 15. Paul R, Jaeger T, Abel S, Wiederkehr I, Folcher M, Biondi EG, Laub MT, Jenal  
905 U. 2008. Allosteric regulation of histidine kinases by their cognate response  
906 regulator determines cell fate. *Cell* 133:452-61.

- 907 16. Abel S, Chien P, Wassmann P, Schirmer T, Kaefer V, Laub MT, Baker TA,  
908 Jenal U. 2011. Regulatory cohesion of cell cycle and cell differentiation  
909 through interlinked phosphorylation and second messenger networks. *Mol Cell*  
910 43:550-60.
- 911 17. Duerig A, Abel S, Folcher M, Nicollier M, Schwede T, Amiot N, Giese B, Jenal  
912 U. 2009. Second messenger-mediated spatiotemporal control of protein  
913 degradation regulates bacterial cell cycle progression. *Genes Dev* 23:93-104.
- 914 18. Smith SC, Joshi KK, Zik JJ, Trinh K, Kamajaya A, Chien P, Ryan KR. 2014.  
915 Cell cycle-dependent adaptor complex for ClpXP-mediated proteolysis directly  
916 integrates phosphorylation and second messenger signals. *Proc Natl Acad Sci*  
917 *U S A* 111:14229-34.
- 918 19. Stock AM, Robinson VL, Goudreau PN. 2000. Two-component signal  
919 transduction. *Annu Rev Biochem* 69:183-215.
- 920 20. Matroule JY, Lam H, Burnette DT, Jacobs-Wagner C. 2004. Cytokinesis  
921 monitoring during development; rapid pole-to-pole shuttling of a signaling  
922 protein by localized kinase and phosphatase in *Caulobacter*. *Cell* 118:579-90.
- 923 21. Hung DY, Shapiro L. 2002. A signal transduction protein cues proteolytic  
924 events critical to *Caulobacter* cell cycle progression. *Proc Natl Acad Sci U S A*  
925 99:13160-5.
- 926 22. Iniesta AA, Shapiro L. 2008. A bacterial control circuit integrates polar  
927 localization and proteolysis of key regulatory proteins with a phospho-signaling  
928 cascade. *Proc Natl Acad Sci U S A* 105:16602-7.
- 929 23. Wang SP, Sharma PL, Schoenlein PV, Ely B. 1993. A histidine protein kinase  
930 is involved in polar organelle development in *Caulobacter crescentus*. *Proc*  
931 *Natl Acad Sci U S A* 90:630-4.
- 932 24. Ardisson S, Fumeaux C, Berge M, Beaussart A, Theraulaz L, Radhakrishnan  
933 SK, Dufrene YF, Viollier PH. 2014. Cell cycle constraints on capsulation and  
934 bacteriophage susceptibility. *Elife* 3.
- 935 25. Fumeaux C, Radhakrishnan SK, Ardisson S, Theraulaz L, Frandi A, Martins  
936 D, Nesper J, Abel S, Jenal U, Viollier PH. 2014. Cell cycle transition from S-  
937 phase to G1 in *Caulobacter* is mediated by ancestral virulence regulators. *Nat*  
938 *Commun* 5:4081.
- 939 26. Lagenaur C, Farmer S, Agabian N. 1977. Adsorption properties of stage-  
940 specific *Caulobacter* phage phiCbK. *Virology* 77:401-7.
- 941 27. Edwards P, Smit J. 1991. A transducing bacteriophage for *Caulobacter*  
942 *crescentus* uses the paracrystalline surface layer protein as a receptor. *J*  
943 *Bacteriol* 173:5568-72.
- 944 28. Radhakrishnan SK, Thanbichler M, Viollier PH. 2008. The dynamic interplay  
945 between a cell fate determinant and a lysozyme homolog drives the  
946 asymmetric division cycle of *Caulobacter crescentus*. *Genes Dev* 22:212-25.
- 947 29. Bodenmiller D, Toh E, Brun YV. 2004. Development of surface adhesion in  
948 *Caulobacter crescentus*. *J Bacteriol* 186:1438-47.

- 949 30. Jacobs C, Ausmees N, Cordwell SJ, Shapiro L, Laub MT. 2003. Functions of  
950 the CckA histidine kinase in *Caulobacter* cell cycle control. *Mol Microbiol*  
951 47:1279-90.
- 952 31. Delaby M, Panis G, Viollier PH. 2019. Bacterial cell cycle and growth phase  
953 switch by the essential transcriptional regulator CtrA. *Nucleic Acids Res*  
954 47:10628-10644.
- 955 32. Vass RH, Zeinert RD, Chien P. 2016. Protease regulation and capacity during  
956 *Caulobacter* growth. *Curr Opin Microbiol* 34:75-81.
- 957 33. McGrath PT, Iniesta AA, Ryan KR, Shapiro L, McAdams HH. 2006. A  
958 dynamically localized protease complex and a polar specificity factor control a  
959 cell cycle master regulator. *Cell* 124:535-47.
- 960 34. Aakre CD, Phung TN, Huang D, Laub MT. 2013. A bacterial toxin inhibits DNA  
961 replication elongation through a direct interaction with the beta sliding clamp.  
962 *Mol Cell* 52:617-28.
- 963 35. Radhakrishnan SK, Pritchard S, Viollier PH. 2010. Coupling prokaryotic cell  
964 fate and division control with a bifunctional and oscillating oxidoreductase  
965 homolog. *Dev Cell* 18:90-101.
- 966 36. Bhat NH, Vass RH, Stoddard PR, Shin DK, Chien P. 2013. Identification of  
967 ClpP substrates in *Caulobacter crescentus* reveals a role for regulated  
968 proteolysis in bacterial development. *Mol Microbiol* 88:1083-92.
- 969 37. Beaufay F, Coppine J, Mayard A, Laloux G, De Bolle X, Hallez R. 2015. A  
970 NAD-dependent glutamate dehydrogenase coordinates metabolism with cell  
971 division in *Caulobacter crescentus*. *EMBO J* 34:1786-800.
- 972 38. Kaczmarczyk A, Hempel AM, von Arx C, Bohm R, Dubey BN, Nesper J,  
973 Schirmer T, Hiller S, Jenal U. 2020. Precise timing of transcription by c-di-  
974 GMP coordinates cell cycle and morphogenesis in *Caulobacter*. *Nat Commun*  
975 11:816.
- 976 39. Chen JC, Viollier PH, Shapiro L. 2005. A membrane metalloprotease  
977 participates in the sequential degradation of a *Caulobacter* polarity  
978 determinant. *Mol Microbiol* 55:1085-103.
- 979 40. Janakiraman B, Mignolet J, Narayanan S, Viollier PH, Radhakrishnan SK.  
980 2016. In-phase oscillation of global regulons is orchestrated by a pole-specific  
981 organizer. *Proc Natl Acad Sci U S A* 113:12550-12555.
- 982 41. Paul R, Weiser S, Amiot NC, Chan C, Schirmer T, Giese B, Jenal U. 2004.  
983 Cell cycle-dependent dynamic localization of a bacterial response regulator  
984 with a novel di-guanylate cyclase output domain. *Genes Dev* 18:715-27.
- 985 42. Hsing W, Silhavy TJ. 1997. Function of conserved histidine-243 in  
986 phosphatase activity of EnvZ, the sensor for porin osmoregulation in  
987 *Escherichia coli*. *J Bacteriol* 179:3729-35.
- 988 43. Lori C, Kaczmarczyk A, de Jong I, Jenal U. 2018. A Single-Domain Response  
989 Regulator Functions as an Integrating Hub To Coordinate General Stress  
990 Response and Development in Alphaproteobacteria. *mBio* 9.
- 991 44. Lourenco RF, Kohler C, Gomes SL. 2011. A two-component system, an anti-  
992 sigma factor and two paralogous ECF sigma factors are involved in the control

- 993 of general stress response in *Caulobacter crescentus*. *Mol Microbiol* 80:1598-  
994 612.
- 995 45. Foreman R, Fiebig A, Crosson S. 2012. The LovK-LovR two-component  
996 system is a regulator of the general stress pathway in *Caulobacter crescentus*.  
997 *J Bacteriol* 194:3038-49.
- 998 46. Kaczmarczyk A, Campagne S, Danza F, Metzger LC, Vorholt JA, Francez-  
999 Charlot A. 2011. Role of *Sphingomonas* sp. strain Fr1 PhyR-NepR-sigmaEcfG  
1000 cascade in general stress response and identification of a negative regulator  
1001 of PhyR. *J Bacteriol* 193:6629-38.
- 1002 47. Kaczmarczyk A, Vorholt JA, Francez-Charlot A. 2013. Cumate-inducible gene  
1003 expression system for sphingomonads and other Alphaproteobacteria. *Appl*  
1004 *Environ Microbiol* 79:6795-802.
- 1005 48. Gottschlich L, Bortfeld-Miller M, Gabelein C, Dintner S, Vorholt JA. 2018.  
1006 Phosphorelay through the bifunctional phosphotransferase PhyT controls the  
1007 general stress response in an alphaproteobacterium. *PLoS Genet*  
1008 14:e1007294.
- 1009 49. Joshi KK, Berge M, Radhakrishnan SK, Viollier PH, Chien P. 2015. An  
1010 Adaptor Hierarchy Regulates Proteolysis during a Bacterial Cell Cycle. *Cell*  
1011 163:419-31.
- 1012 50. Gorbatyuk B, Marczynski GT. 2005. Regulated degradation of chromosome  
1013 replication proteins DnaA and CtrA in *Caulobacter crescentus*. *Mol Microbiol*  
1014 55:1233-45.
- 1015 51. Ronneau S, Petit K, De Bolle X, Hallez R. 2016. Phosphotransferase-  
1016 dependent accumulation of (p)ppGpp in response to glutamine deprivation in  
1017 *Caulobacter crescentus*. *Nat Commun* 7:11423.
- 1018 52. Hallez R, Bellefontaine AF, Letesson JJ, De Bolle X. 2004. Morphological and  
1019 functional asymmetry in alpha-proteobacteria. *Trends Microbiol* 12:361-5.
- 1020 53. Hallez R, Mignolet J, Van Mullem V, Wery M, Vandenhoute J, Letesson JJ,  
1021 Jacobs-Wagner C, De Bolle X. 2007. The asymmetric distribution of the  
1022 essential histidine kinase PdhS indicates a differentiation event in *Brucella*  
1023 *abortus*. *EMBO J* 26:1444-55.
- 1024 54. Brillì M, Fondi M, Fani R, Mengoni A, Ferri L, Bazzicalupo M, Biondi EG. 2010.  
1025 The diversity and evolution of cell cycle regulation in alpha-proteobacteria: a  
1026 comparative genomic analysis. *BMC Syst Biol* 4:52.
- 1027 55. Kim J, Heindl JE, Fuqua C. 2013. Coordination of division and development  
1028 influences complex multicellular behavior in *Agrobacterium tumefaciens*. *PLoS*  
1029 *One* 8:e56682.
- 1030 56. Pini F, Frage B, Ferri L, De Nisco NJ, Mohapatra SS, Taddei L, Fioravanti A,  
1031 Dewitte F, Galardini M, Brillì M, Villeret V, Bazzicalupo M, Mengoni A, Walker  
1032 GC, Becker A, Biondi EG. 2013. The DivJ, CbrA and PleC system controls  
1033 DivK phosphorylation and symbiosis in *Sinorhizobium meliloti*. *Mol Microbiol*  
1034 90:54-71.
- 1035 57. Sadowski CS, Wilson D, Schallies KB, Walker G, Gibson KE. 2013. The  
1036 *Sinorhizobium meliloti* sensor histidine kinase CbrA contributes to free-living  
1037 cell cycle regulation. *Microbiology* 159:1552-1563.

- 1038 58. Heindl JE, Crosby D, Brar S, Pinto JF, Singletary T, Merenich D, Eagan JL,  
1039 Buechlein AM, Bruger EL, Waters CM, Fuqua C. 2019. Reciprocal control of  
1040 motility and biofilm formation by the PdhS2 two-component sensor kinase of  
1041 *Agrobacterium tumefaciens*. *Microbiology* 165:146-162.
- 1042 59. Francis N, Poncin K, Fioravanti A, Vassen V, Willemart K, Ong TA, Rappez L,  
1043 Letesson JJ, Biondi EG, De Bolle X. 2017. CtrA controls cell division and outer  
1044 membrane composition of the pathogen *Brucella abortus*. *Mol Microbiol*  
1045 103:780-797.
- 1046 60. Ely B. 1991. Genetics of *Caulobacter crescentus*. *Methods Enzymol* 204:372-  
1047 84.
- 1048 61. Ronneau S, Caballero-Montes J, Coppine J, Mayard A, Garcia-Pino A, Hallez  
1049 R. 2019. Regulation of (p)ppGpp hydrolysis by a conserved archetypal  
1050 regulatory domain. *Nucleic Acids Res* 47:843-854.
- 1051 62. Pini F, De Nisco NJ, Ferri L, Penterman J, Fioravanti A, Brillì M, Mengoni A,  
1052 Bazzicalupo M, Viollier PH, Walker GC, Biondi EG. 2015. Cell Cycle Control  
1053 by the Master Regulator CtrA in *Sinorhizobium meliloti*. *PLoS Genet*  
1054 11:e1005232.
- 1055 63. Li H, Durbin R. 2009. Fast and accurate short read alignment with Burrows-  
1056 Wheeler transform. *Bioinformatics* 25:1754-60.
- 1057 64. Li H, Handsaker B, Wysoker A, Fennell T, Ruan J, Homer N, Marth G,  
1058 Abecasis G, Durbin R, Genome Project Data Processing S. 2009. The  
1059 Sequence Alignment/Map format and SAMtools. *Bioinformatics* 25:2078-9.
- 1060 65. Zhang Y, Liu T, Meyer CA, Eeckhoute J, Johnson DS, Bernstein BE,  
1061 Nusbaum C, Myers RM, Brown M, Li W, Liu XS. 2008. Model-based analysis  
1062 of ChIP-Seq (MACS). *Genome Biol* 9:R137.
- 1063

1064 **Figure legends**

1065 **Figure 1:** CtrA regulation pathway in *Caulobacter crescentus* in (a) swarmer and (b)  
1066 stalked cells. In swarmer cells (a), DivK is actively dephosphorylated by PleC and  
1067 CckN, and therefore not able to interact with DivL. Free DivL activates the  
1068 phosphorelay culminating in CtrA and CpdR phosphorylation. Active CtrA (CtrA~P)  
1069 regulates the expression of more than 200 genes and inhibits DNA replication  
1070 initiation by binding the single chromosomal origin of replication (*Cori*). At the G1-S  
1071 transition (b), CckN and PleC are cleared from the cells while DivK and PleD are  
1072 phosphorylated by their cognate histidine kinase DivJ. Phosphorylated DivK (DivK~P)  
1073 interacts with DivL and reduces its affinity for CckA leading to an inhibition of its  
1074 kinase activity on CtrA and CpdR. Phosphorylation of PleD promotes its diguanylate  
1075 cyclase activity resulting in an increased synthesis of c-di-GMP. High levels of c-di-  
1076 GMP not only stimulates CckA phosphatase activity on both CpdR~P and CtrA~P,  
1077 but also drives, concomitantly with unphosphorylated CpdR, ClpXP-dependent  
1078 degradation of CtrA. Together, this results in the rapid inactivation of CtrA allowing  
1079 DNA replication initiation to proceed.

1080

1081 **Figure 2:** CckN is a phosphatase for DivK and PleD. (a) Co-immunoprecipitation  
1082 (Co-IP) experiments showing that CckN and DivK are part of the same protein  
1083 complex. Co-IP were performed on protein extracts of *cckN-TwinStrep* (RH2235) and  
1084 wild-type (RH2070) strains. CckN and DivK were detected by Western blotting using  
1085 respectively anti-CckN and anti-DivK antibodies before (Input) and after  
1086 immunoprecipitation (IP) with Strep-Tactin coated magnetic beads. CckN-TS: CckN-  
1087 TwinStrep (b) Bacterial two-hybrid assay showing that CckN and DivK interact with  
1088 each other.  $\beta$ -galactosidase assays were performed on MG1655 *cyaA::frt* (RH785)  
1089 strains coexpressing T18 fused to *ZIP*, *cckN*, or *divK* with T25 fused to *ZIP*, *cckN*, or  
1090 *divK*. T18 and T25 alone were used as negative controls while coexpression of T18-  
1091 *ZIP* and T25-*ZIP* was used as a positive control. Error bars = SD,  $n \geq 3$ . (c) *In vitro*  
1092 phosphorylation assay showing that CckN cannot phosphorylate DivK but can  
1093 dephosphorylate DivK~P. CckN or DivJ<sup>Sm</sup> was incubated alone for 40' with [ $\gamma$ -  
1094 <sup>32</sup>P]ATP before adding DivK for 15'. Then, DivK phosphorylated by DivJ<sup>Sm</sup> was  
1095 washed to remove excess of [ $\gamma$ -<sup>32</sup>P]ATP (dotted line) and incubated with or without  
1096 CckN for the indicated time. (d) *In vitro* phosphorylation assay showing that CckN

1097 can dephosphorylate PleD~P. DivJ was incubated alone for 1h with [ $\gamma$ -<sup>32</sup>P]ATP  
1098 before adding PleD for 2' before adding CckN or buffer incubating for the indicated  
1099 time. DivJ\* likely corresponds to a degradation product of DivJ (e) *In vivo*  
1100 phosphorylation assay showing that overexpression of functional *cckN* decreases of  
1101 PleD phosphorylation. Wild-type (RH50) cells harbouring the pBX, pBX-*cckN* or  
1102 *cckN*<sub>H47A</sub> plasmid were grown for 3 h in M5G with 0.05 mM phosphate supplemented  
1103 with 0.1% xylose. The phosphorylation (up) and protein (down) levels of PleD were  
1104 determined *in vivo* as described in the Material & Methods.

1105

1106 **Figure 3:** CckN controls development by regulating CtrA activity. (a)  $\beta$ -  
1107 galactosidase assays were performed on wild-type (RH50),  $\Delta divJ \Delta pleC$  (RH1103)  
1108 and  $\Delta divJ \Delta pleC \Delta cckN$  (RH1111) strains harbouring *lacZ* fusions to CtrA-dependent  
1109 ( $P_{sciP}$ ,  $P_{CC1128}$ ,  $P_{CC2199}$  and  $P_{tacA}$ ) and CtrA independent ( $P_{CC3574}$ ) promoters, grown in  
1110 complex medium (PYE) and normalized to the WT (100%). Error bars = SD, n = 4.  
1111 (b) The protein and the phosphorylation levels of CtrA were measured in wild-type  
1112 (RH50),  $\Delta divJ \Delta pleC$  (RH1103) and  $\Delta divJ \Delta pleC \Delta cckN$  (RH1111) strains and  
1113 normalized to the WT (100%). The CtrA protein levels normalized to the MreB levels  
1114 (black bars) were determined by western blotting. The CtrA phosphorylation levels  
1115 (yellow bars) were determined *in vivo* as described in the Material & Methods. The  
1116 CtrA~P/CtrA ratio (red bars) were obtained by dividing black values by yellow values.  
1117 Error bars = SD, n = 3. (c) Bacteriophages sensitivity assays were performed with  
1118 CbK and Cr30 on wild-type (RH50),  $\Delta pleC$  (RH217),  $\Delta cckN$  (RH1106),  $\Delta divJ \Delta pleC$   
1119 (RH1103) and  $\Delta divJ \Delta pleC \Delta cckN$  (RH1111) strains on PYE agar plates. (d)  $\beta$ -  
1120 galactosidase assays were performed on wild-type (RH50),  $\Delta pleC$  (RH217),  $\Delta cckN$   
1121 (RH1106),  $\Delta divJ \Delta pleC$  (RH1103),  $\Delta divJ \Delta pleC \Delta cckN$  (RH1111) and  
1122  $\Delta divJ \Delta pleC cckN_{H47A}$  (RH1800) strains harbouring  $P_{pilA}::lacZ$  or  $P_{hvyA}::lacZ$  fusions,  
1123 grown in complex medium (PYE) and normalized to the WT (100%). Error bars = SD,  
1124 n = 3. (e) Buoyancy was evaluated by mixing 550  $\mu$ l of Ludox LS Colloidal Silica  
1125 (30%) to 1 ml of wild-type (RH50),  $\Delta pleC$  (RH217),  $\Delta cckN$  (RH1106),  $\Delta divJ \Delta pleC$   
1126 (RH1103) and  $\Delta divJ \Delta pleC \Delta cckN$  (RH1111) strains grown in PYE. Then, the mix  
1127 was centrifuged for 15 min at 9,000 rpm. (f) Cr30-dependent transduction efficiency  
1128 was measured by transducing Cr30 lysates (LHR73 or LHR75) in wild-type (RH50),  
1129  $\Delta pleC$  (RH217),  $\Delta cckN$  (RH1106),  $\Delta divJ \Delta pleC$  (RH1103),  $\Delta divJ \Delta pleC \Delta cckN$

1130 (RH1111) and  $\Delta divJ \Delta pleC cckN_{H47A}$  (RH1800) strains grown in complex medium  
1131 (PYE) and normalized to the WT (100%). Error bars = SD, n = 2. Means were  
1132 statistically compared using a two-way ANOVA (panels a, b and d) or a one-way  
1133 ANOVA (panel f), followed by Tukey's multiple comparisons test; not significant (ns),  
1134  $P < 0.05$  (\*),  $P < 0.01$  (\*\*),  $P < 0.001$  (\*\*\*),  $P < 0.0001$  (\*\*\*\*).

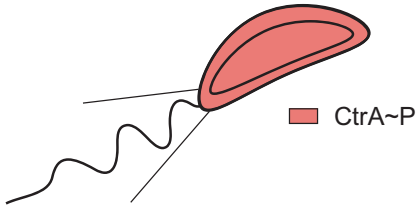
1135  
1136 **Figure 4:** Overexpression of *cckN* leads to a CtrA-dependent toxic G1 block. (a)  
1137 Phase contrast imaging and FACS profiles of wild-type (RH50) cells harbouring  
1138 either the empty pBX vector (EV) or a pBX-*cckN* plasmid grown for 3 h in PYE  
1139 supplemented with 0.1% xylose. (b) Serial dilutions of the wild-type (RH50) strain  
1140 harbouring the empty pBX vector (EV) and the wild-type (RH50), *cckATS1* (RH340),  
1141 *ctrA401* (RH212), *cpdR<sub>D51A</sub>* (RH347), *cpdR<sub>D51A</sub>  $\Delta divK::aacC1$*  (RH1411) strains  
1142 harbouring pBXMCS-2-*cckN* grown in PYE were spotted on PYE (left) or PYE  
1143 supplemented with 0.1% xylose (right) and incubated for 2 days at 30° C. (c) Serial  
1144 dilutions of the *cckN::nptII* strain harbouring the empty pQF vector (EV) or pQF  
1145 vector expressing *cckN* variants grown in PYE were spotted on PYE (left) or PYE  
1146 supplemented with 100  $\mu$ M cumate (right) and incubated for 2 days at 30° C.

1147  
1148 **Figure 5:** The ClpXP protease is responsible for the cell cycle oscillation of CckN  
1149 and PleC. (a) Immunoblotting of protein samples extracted from synchronized *cckN*-  
1150 *3FLAG* (RH1881) or *3FLAG-CckN* (RH1929) cells to follow CckN, CtrA and MreB  
1151 abundance throughout the cell cycle. The time at which the samples were withdrawn  
1152 after synchrony are indicated in minutes. (b) The relative abundance of CckN-  
1153 *3FLAG*, PleC and CtrA was measured in wild-type (RH50 or RH1881),  $\Delta socAB$   
1154 (RH1671 or RH737),  $\Delta socAB \Delta clpP$  (RH2279 or RH1063),  $\Delta socAB \Delta clpX$  (RH1674  
1155 or RH995),  $\Delta clpA$  (RH864 or RH1093),  $\Delta lon$  (RH2472 or RH1228),  $\Delta hslV$  (RH864 or  
1156 RH1247),  $\Delta ftsH$  (RH865 or RH1229),  $\Delta cpdR$  (RH339 or RH1133),  $\Delta rcdA$  (RH323 or  
1157 RH1149) and  $\Delta popA$  (RH315 or RH1151). Means were statistically compared using a  
1158 two-way ANOVA, followed by Dunnett's multiple comparisons test; not significant  
1159 (ns),  $P < 0.01$  (\*\*),  $P < 0.0001$  (\*\*\*\*). (c) The relative abundance of CckN-*3FLAG* and  
1160 PleC and CtrA was measured in wild-type (RH1881), *3FLAG-cckN* (RH1929),  
1161 *cckN<sub>AA::DD</sub>-3FLAG* (RH1576) and *pleC<sub>AA::DD</sub>* (RH2548) strains grown in complex  
1162 medium (PYE) and normalized to the corresponding WT (100%). Error bars = SD, n

1163 = 3. Means were statistically compared using a one-way ANOVA, followed by Sidak's  
1164 multiple comparisons; not significant (ns),  $P < 0.0001$  (\*\*\*\*). Only significant  
1165 differences are indicated on the graph.

Figure 1

a



b

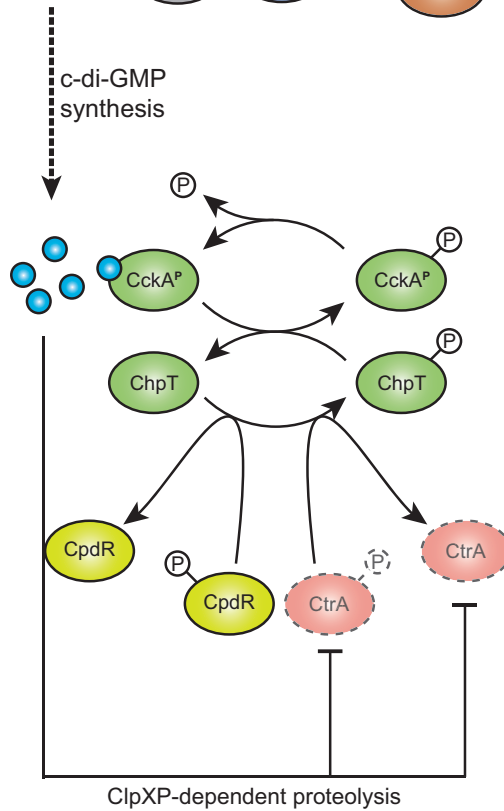
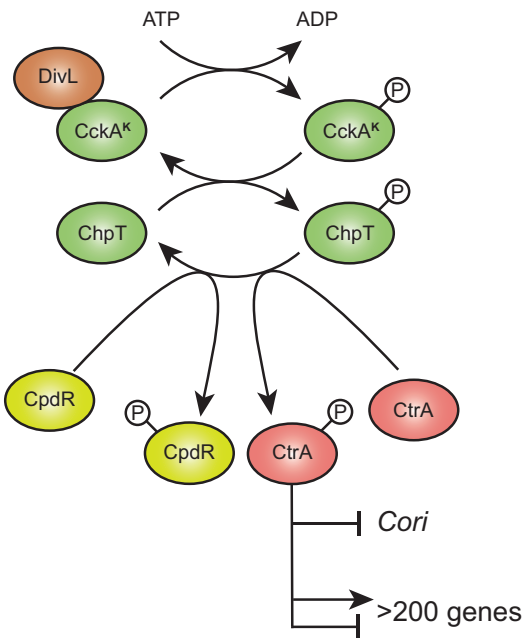
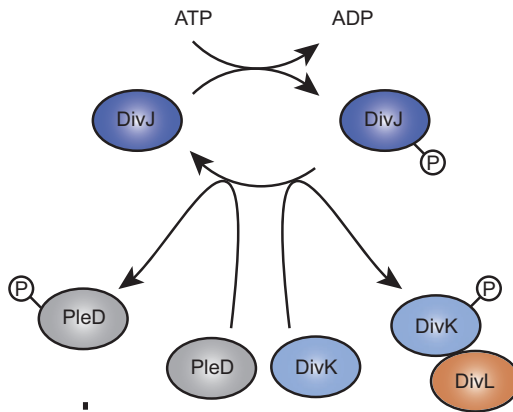
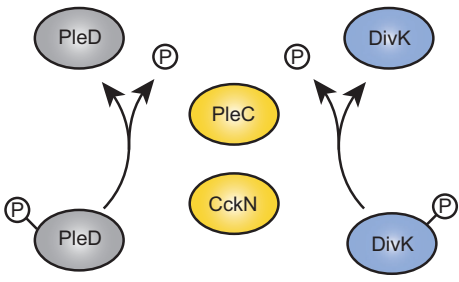
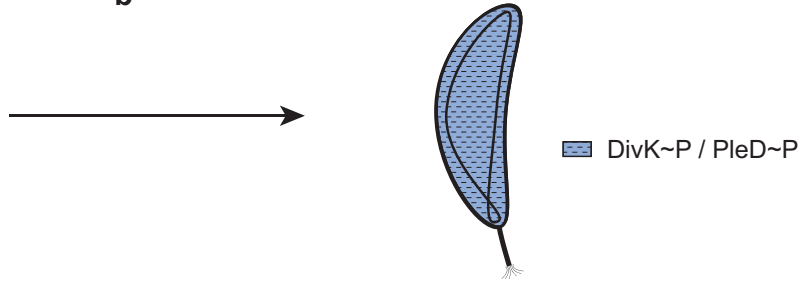


Figure 2

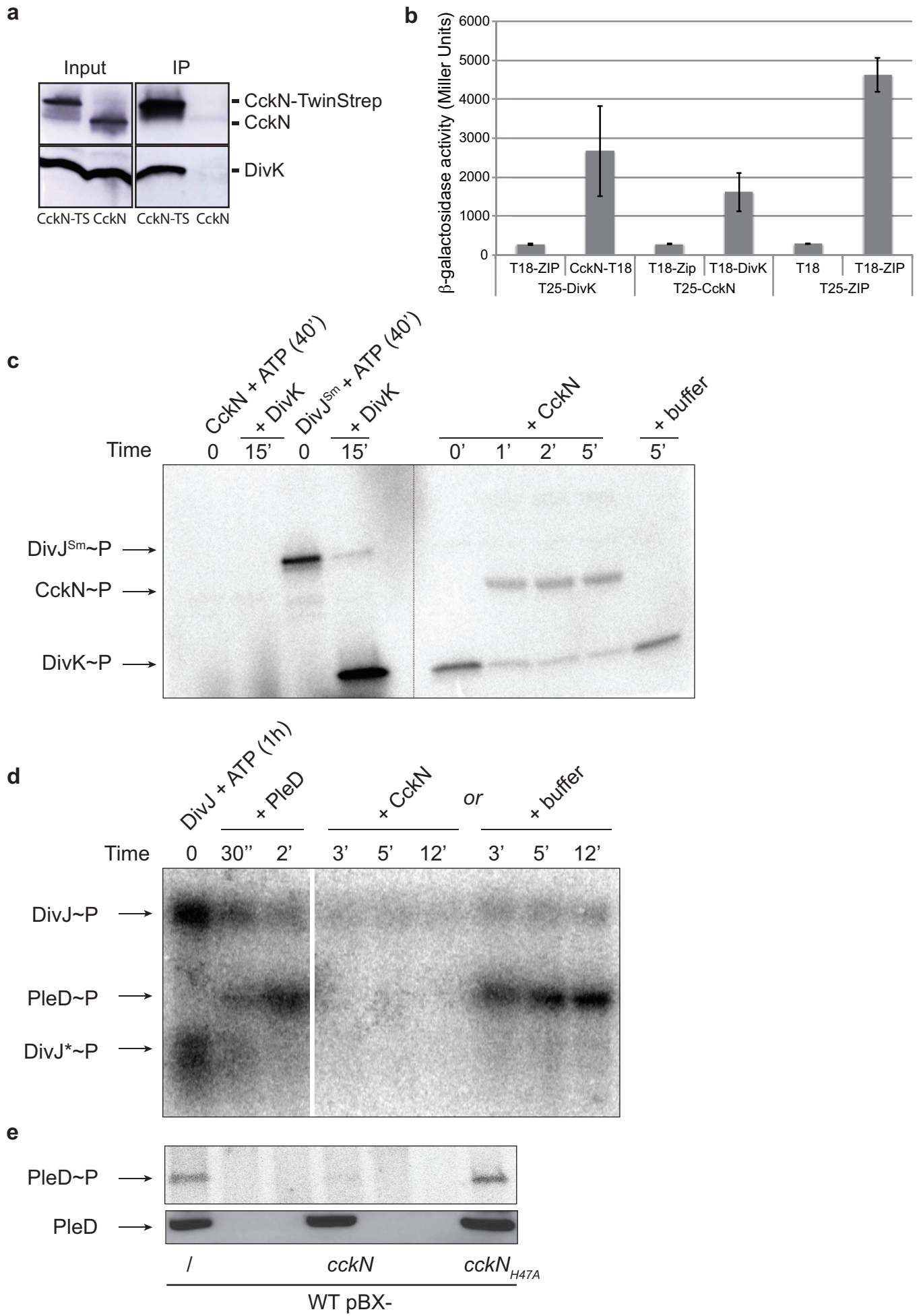


Figure 3

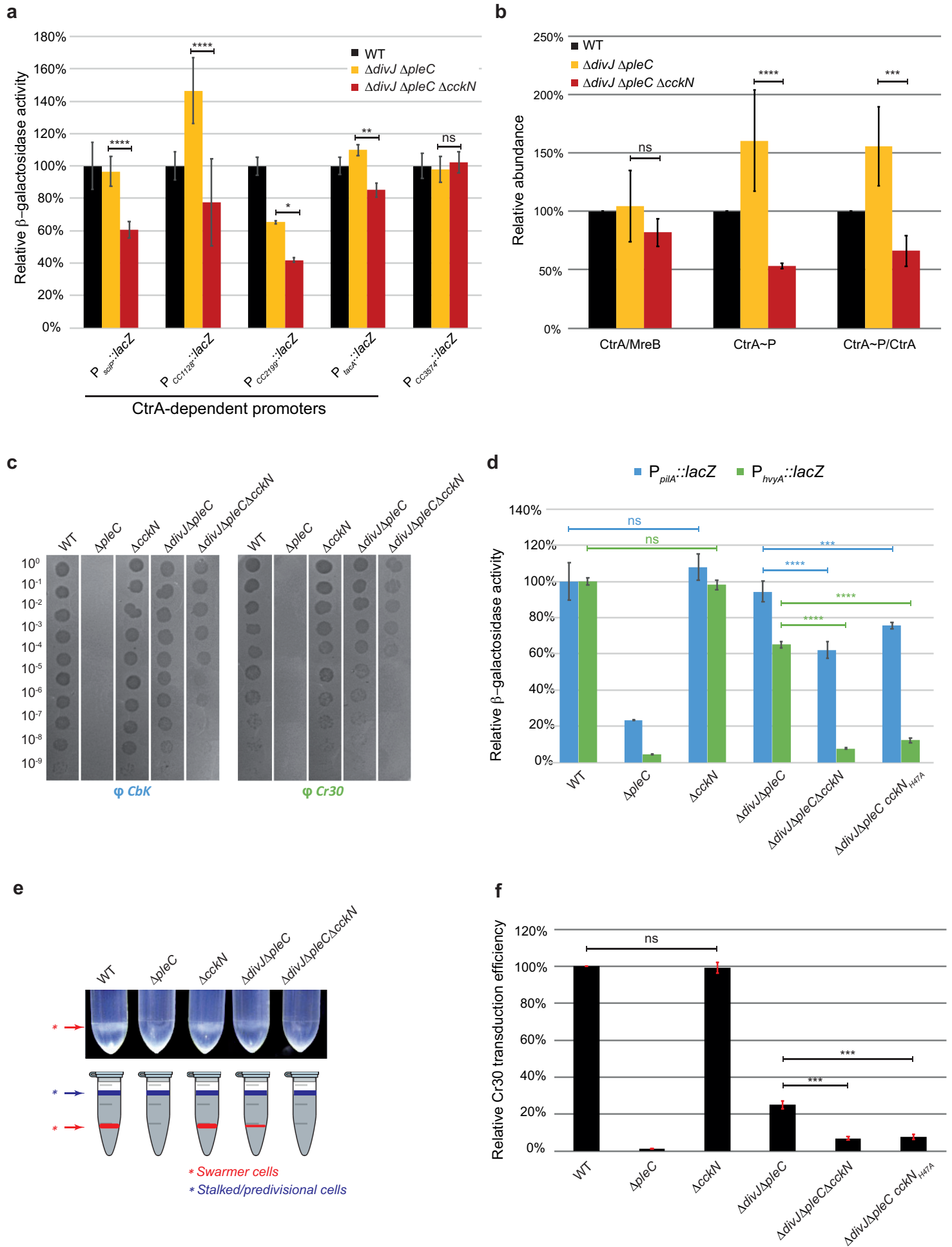
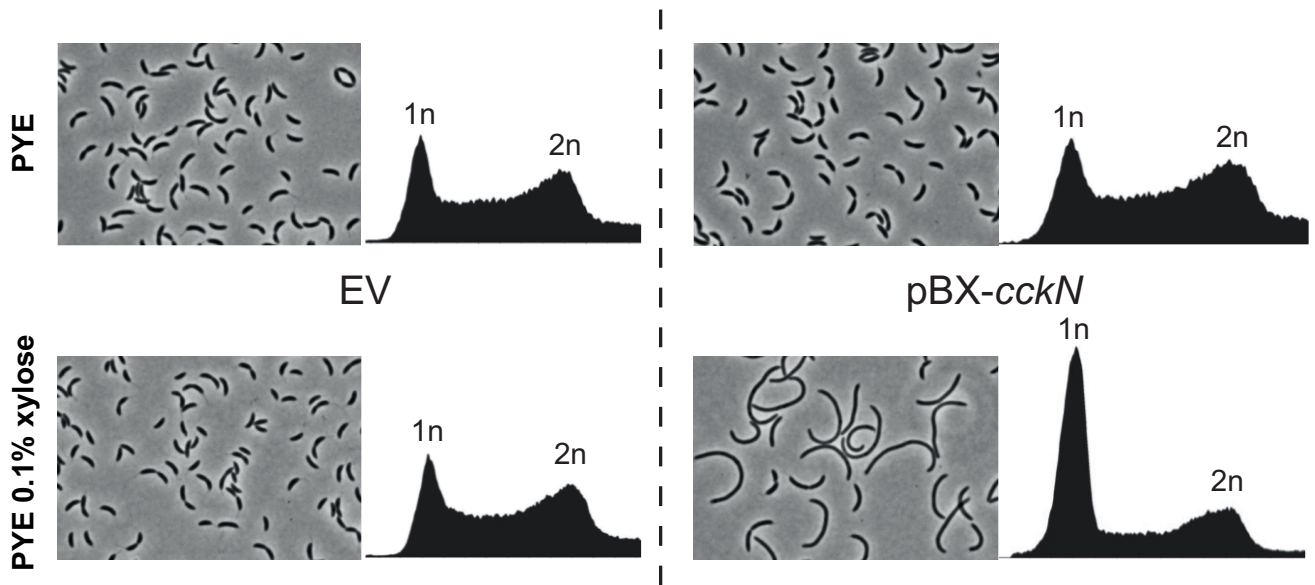
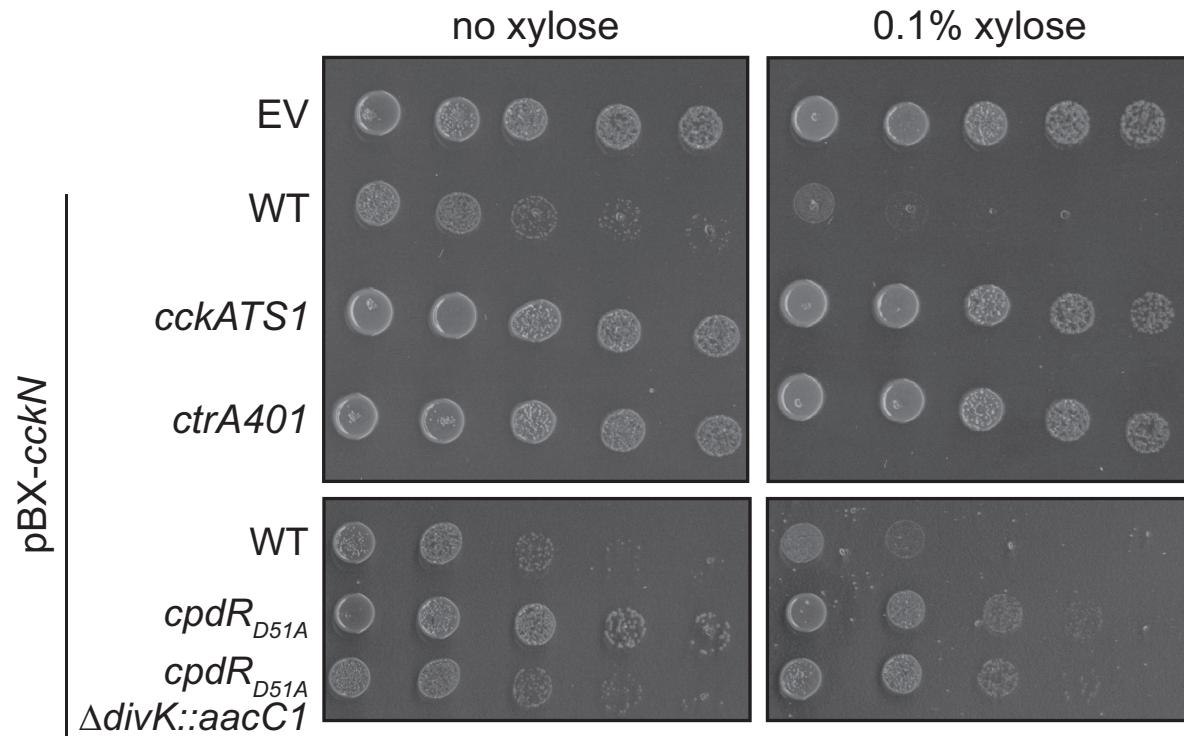


Figure 4

**a**



**b**



**c**

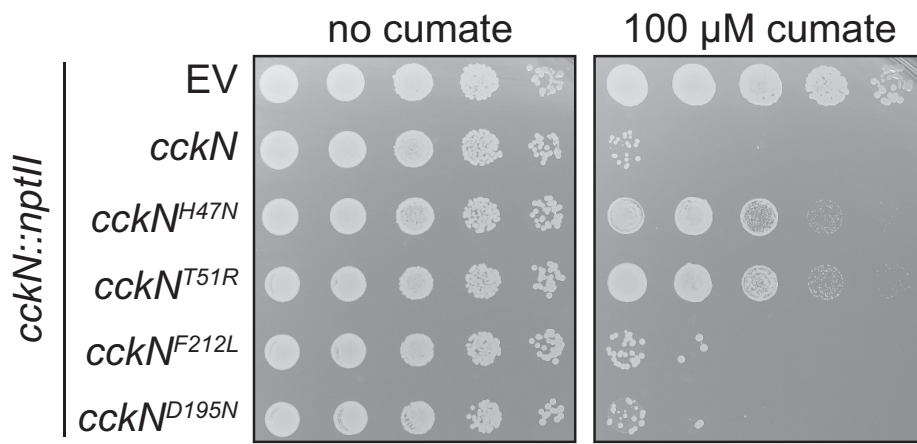


Figure 5

